UNIVERSITÀ DEGLI STUDI DI PADOVA

Dipartimento di Scienze Chimiche

CORSO DI LAUREA MAGISTRALE IN CHIMICA INDUSTRIALE

TESI DI LAUREA MAGISTRALE

Design and synthesis of organic charge selective layers for perovskite solar cells based on extended pi-conjugated molecules

Laureando:

Lorenzo Capone

Relatore:

Prof. Enzo Menna

Correlatore:

Prof. Nazario Martín (UCM)

Controrelatore:

Prof. Diego Frezzato

ANNO ACCADEMICO 2022/2023

Per aspera ad astra

INDEX

ACRONYMS AND ABBREVIATIONS

Ac	Acetate
AIE	Aggregation-Induced Emission
DCC	N,N′-Dicyclohexylcarbodiimide
DCE	Dichloroethane
DCM	Dichloromethane
DDQ	2,3-Dichloro-5,6-dicyano-1,4-benzoquinone
DMAP	4-Dimethylaminopyridine
DMF	Dimethylformamide
ETL	Electron Transport Layer
ETM	Electron Transport Material
EtOH	Ethanol
FT	Fourier Transform
GHGs	Greenhouse gasses
GQD	Graphene Quantum Dot
HBC	Hexa-peri-hexabenzocoronene
HOMO	Highest Occupied Molecular Orbital
HPB	Hexaphenylbenzene
HTL	Hole Transport Layer
HTM	Hole Transport Material
IPCC	Intergovernmental Panel on Climate Change
IR	Infrared
ITO	Indium-tin Oxide
LUMO	Lowest Unoccupied Molecular Orbital
MALDI–TOF MS	Matrix-Assisted Laser Desorption Ionization–Time Of Flight Mass Spectrometry
MeOH	Methanol
NG	Nanographene
NMR	Nuclear Magnetic Resonance
o-DCB	Orto Dichlorobenzene
OLED	Organic Light Emitting Diode
PSC	Perovskite Solar Cell
PVC	Photovoltaics Cell

THF	Tetrahydrofuran
TLC	Thin Layer Chromatography
TMSA	Ethynyltrimethylsilane
UV-Vis	Ultraviolet-Visible

1 INTRODUCTION

1.1 Climate change

We are living a very peculiar historical time, where technologies are very developed and still, we have a lot of potential to develop. At the same time, the conditions where we are living in are pushing us to improve our lifestyles and everything is connected to it.

Speaking of which, a very huge problematic is the climate change that is challenging us on a scientific and more on a social side. This is why we have different (and too many) definitions of it and as many solutions to this problem.

The scientifically most relevant definition is given by the Intergovernmental Panel on Climate Change (IPCC): *Any change in climate over time whether due to natural variability or as a result of human activity*.[1] In the light of this, the society must be able to overcome every natural change of the global climate and also be able to fight against the changes that the human being is causing with their lifestyle.

This lifestyle is allowed by the huge use of fossil fuels since the industrial revolution. In fact, these are the driving forces of global economy not only from an energetic point of view and now more than 80% of the energy needed comes from them.[2]

This exploitation of fossil fuels leads to some problems. The first one is the depletion of source of fuel: deposits are limited in both quantity and capacity. Having said that, no studies have yet proved that the fossil fuels are running out in the next century.

Then, we have to focus on the several negative impacts that are related to the massive use of fossil fuels. In fact, the combustion of these is the cause of local air pollution which seems to be linked to premature deaths and also to the production of greenhouse gasses (GHGs).[3]

1.2 Fossil fuels

But what are fossil fuels? Fuel is defined as material that can be worked to release energy in a controlled way in form of heat or work. Fossil fuels are fossilised

biomass which has stored carbon through time and once combusted releases this carbon into the atmosphere mainly in form of CO_2.[4]

1.3 Greenhouse gasses

And what are GHGs? They are IR active gasses like water vapor, carbon dioxide and ozone. They are naturally present in the atmosphere and they have the role of absorbing thermal IR radiation coming from Earth's surface. The atmosphere, once warmed up, emits in turn IR radiation: this is called greenhouse effect.[5]

1.4 Sustainable energies

To reduce GHGs, more sustainable energies were introduced: energy that in its production and consumption, has minimal negative impacts on human health and the healthy functioning of vital ecological systems, including the global environment.[6] And renewable energy is one of them.

Solar energy is the fundamental renewable energy source in nature. It is interesting because it can be practically endless.

One of the problems is that it is difficult to gather data needed in modelling solar energy devices and a good database is required to permit the work of energy planners, engineers and scientists.[6]

1.5 Photovoltaic technology

Nowadays, photovoltaic cells (PVCs) have gained in efficiency and then in importance, thus emerging as a sustainable source of energy with the promise of playing gradually a bigger part in the energy industry.

Silicon technology is well known and widely used, but day by day both organic and organic-inorganic alternatives are growing. Actually, a lot of studies are working on organic devices with different characteristics trying to investigate and improve different features such as energetic yield and durability in time and against environmental factors.[7]

Using an organic device gives the advantage of having features connected with the organic macromolecules. So, flexible plastics can be used as substrates, providing to the device new additional characteristics such as insulating abilities (thermal or even sound) or transparency or colour and so on. In the end,

depending on the final goal, it is possible to have different products based on the same technology being able to give similar performances.

As already said, there are different kind of alternative photovoltaic technologies but generally it is possible to show a general device structure (fig. 1.1).

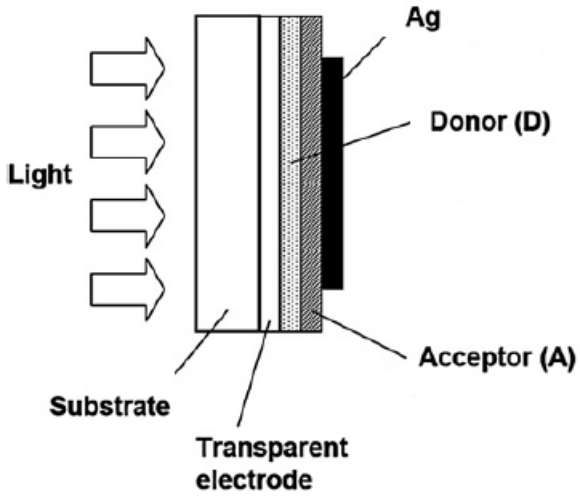

Figure 1.1 – PV device general structure[7]

It consists of a transparent electrode typically based on a conducting oxide such as indium-tin oxide (ITO), two organic light-absorbing layers and a second electrode. These two organic layers are made by two different organic semiconductors with two different roles: one is an electron-donor which exhibits a low ionization potential that is reflected in a high HOMO energy and the other an electron-acceptor which is characterised by a high electron affinity, hence a low LUMO energy. Respectively, these two layers provide for efficiency hole (Hole Transport Layer, HTL) and electron transport (Electron Transport Layer, ETL).[8]

Later, it has been seen that hybrid organic-inorganic devices are more promising than the organic counterpart and specially perovskite solar cells (PSCs). Without saying too much, it is known that the structure of the hybrid device is quite similar to the organic one. A feature of these new devices is the important role of two specific layers: the ETL made by n-type semiconductors and the HTL made by p-type semiconductors.[9]

ETLs are made by electron transport materials (ETMs) which play an important role in a high-performing PSCs. In fact, they extract photogenerated electrons from perovskite and transport these charges to the electrode. At the same time, they serve as a hole blocking layer to supress the charge recombination.

Therefore, high electron mobility is a very important factor because this means that electrons can be efficiently transported and collected. These features can be enhanced by tailoring energy level of these ETMs.[10] In fact, ETMs must satisfy band alignment with the perovskite layer and so they should have LUMO and HOMO higher than the perovskite active layer. In addition, they must present high transmittance in the UV-Vis region so that photons can pass through easily and be absorbed by the perovskite layer.[11]

Instead, HTLs are made by hole transport materials (HTMs) which facilitate hole extraction from the perovskite absorber and transport the holes to the external electrode while blocking the electron movement. For this reason, a characteristic that is required from these materials is high transparency. In addition, other basic requirements for HTMs are firstly a favourable alignment between the HOMO energy level of the HTM and the valence band maximum of the perovskite material, secondly a high mobility for hole transport, then high solubility into an organic solvent and finally good thermal, moisture and chemical stability.[12, 13]

1.5.1 Photovoltaic effect

The working principle of these devices is the photovoltaic effect that is based on photons absorption which induces electron–hole pair formation followed by charge separation in a junction.

More specifically, when the electromagnetic radiation coming from the sun affects the device, an exciton is formed. Within an organic semiconductor, an exciton can be defined as a bound electron–hole pair. However, because of its electroneutrality and the strong binding between the electron and the hole, it is often better described as a mobile excited state (fig. 1.2).[14]

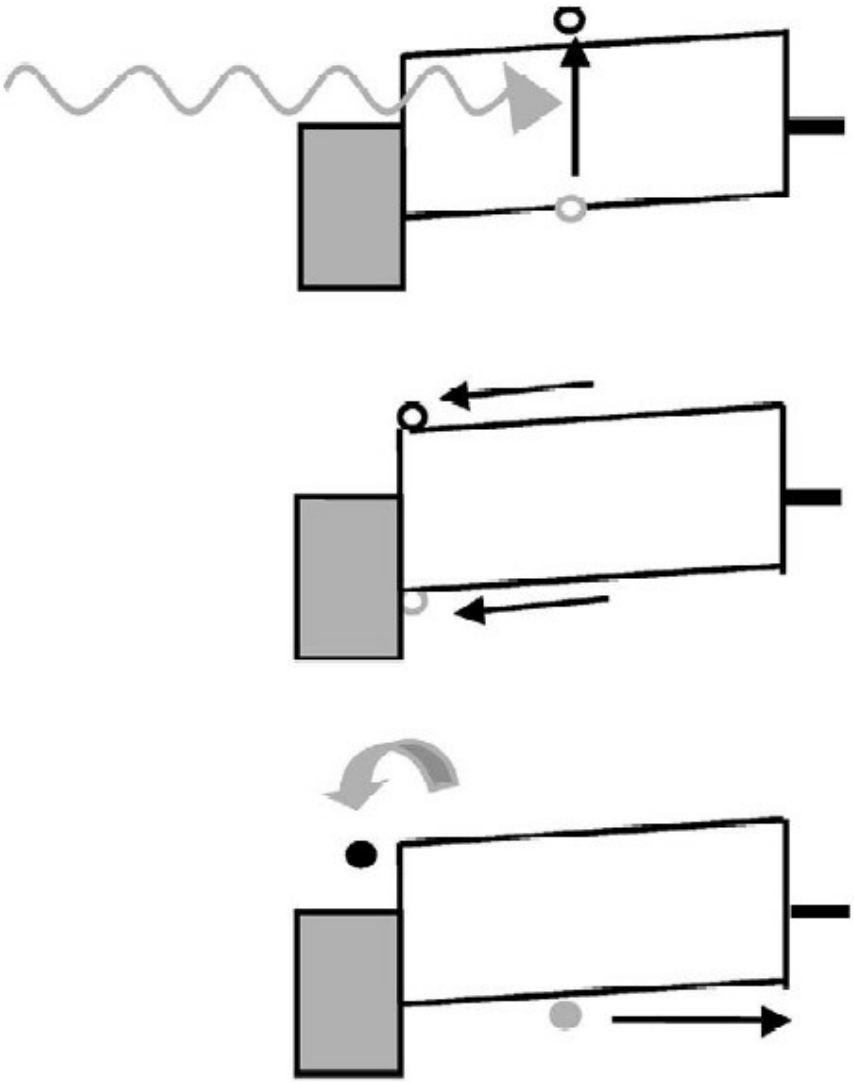

Figure 1.2 – Formation of a exciton caused by solar radiation in an organic conductor connected with two metal contacts. Then, the following hopping to the contact organic layer-metal. Finally the possible dissociation[15]

After its formation, the exciton should reach a dissociation site which could be either a semiconductor/metal or donor/acceptor interface. Unfortunately, excitons in organic materials have a limited diffusion range, usually not exceeding 10 nm, due to low mobility and fast deexcitation processes, meaning that the distance between the formation and the dissociation sites must be within this range.

The charge separation can occur at the interface in-between, namely at either organic semiconductor/metal or organic donor/acceptor interfaces, but in the presence of impurities such as oxygen. The material with larger HOMO – LUMO gap acts as electron acceptor and vice versa the one with smaller HOMO – LUMO gap acts as electron donor (fig. 1.3).

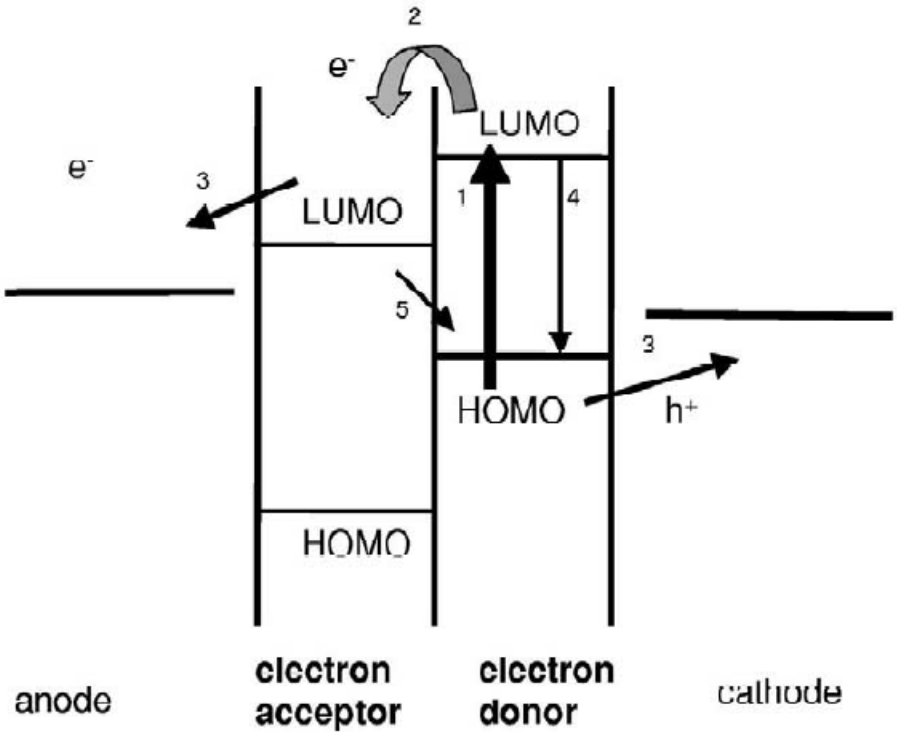

Figure 1.3 – Schematic energy-band diagram of a donor–acceptor[15]

In the figure above, if both excited state (LUMO) and ground state (HOMO) of the donor material lie at energies sufficiently higher than those of the acceptor material, then it is energetically favourable for an exciton reaching the interface to dissociate, leaving a positive polaron on the acceptor and a negative one on the donor. For efficient photocurrent generation, charge separation (2) should compete successfully with geminate recombination (4) after a photon absorption event (1), and transfer to contacts (3) should compete with interfacial recombination (5).[15]

Therefore, to achieve an efficient charge separation we need a difference in energy between the donor LUMO and acceptor LUMO smaller than the exciton energy.

So, due to the slow mobility, these charges can recombine during their path before reaching the electrodes, and this occurs mainly when same material serves as transport medium for both carriers type.[16]

1.5.2 Material characteristics

Regardless of the kind of organic material, all the devices are based on conjugated π electrons. Differently from σ electrons, π ones are more mobile and can move through the alternation of single and double bonds: the so-called

conjugated bonds. These electrons allow organic materials to absorb light, very useful for solar cells, but also to emit, making them perfect for OLEDs.
Molecular π and π* orbitals correspond respectively to the highest occupied molecular orbital and the lowest unoccupied molecular orbital.
The charge transport proceeds by a slower hopping between localised states rather than a faster diffusion within a band (as for inorganic semiconductors, where LUMO and HOMO form conduction and valence bands). Moreover, in the case of polymers and oligomers, both hopping along the conjugated chain and intermolecular charge transport between adjacent chains or molecules occur.[16]
Proper structures for these organic layers are generally characterised by a huge backbone of sp^2 hybridised carbon atoms, or heteroatoms such as nitrogen, oxygen and sulphur, giving rise to π-molecular orbitals. Conjugated orbitals, i.e. delocalised π-orbitals, arise within such structures, with a low HOMO–LUMO energy gap giving rise to proper optical and electrical proprieties.[7]

1.5.3 Organic materials

1.5.3.1 Graphene

Graphene looks like the perfect candidate for this goal and actually it inspired researchers in this field. Graphene is a single atomic layer of graphite, only composed of sp^2 hybridised carbon atoms. It shows a very high electron mobility at room temperature and a very little temperature dependency indeed. This low dependency indicates that electron movement is only hindered by defect scattering. As a result, graphene shows the lowest resistivity between materials.[17]
What makes graphene unsuitable for electronic applications is that the valence and conduction bands slightly overlap making it a zero-bandgap semiconductor, while a band gap is needed for this kind of applications.[18]

1.5.3.2 Nanographenes

For this reason, researchers started to study other carbon allotrope forms such as nanographenes.
Nanographenes (NGs), or graphene quantum dots (GQDs), can be seen as small graphene fragments: NGs and graphene share some interesting characteristics, while more properties can be synthetically modified to fit requirements for the final aim. As it has been said, graphene presents a zero bandgap, NGs instead, show

non-zero bandgap and are mainly governed by their size and edge configurations.[19]

What is interesting in NGs is their nanometre-size and the fact that they are usually semiconductor. Compared to more classical semiconductors, they show a more “molecule-like” character and they are non-toxic, making them much easier to handle. Moreover, they show the electro-optic properties sought by the scientific community.

NGs have a non-zero band gap and show luminesce on excitation. This band gap is tuneable by modifying the size and surface chemistry.

The general absorption spectra shows an important peak at about 230 nm assigned to π→π* excitation of the π-bonds. By functionalising the NG, it is possible to introduce further absorption features and to affect the photoluminescence.[17]

1.6 Main reactions

The chemistry used to synthesise NGs is quite established and simple, allowing to obtain a wide range of products with few main reactions, just adjusting the conditions.

The staple reactions are mainly the next three.

1.6.1 Diels – Alder reaction

One of the key reactions is the Diels – Alder reaction carried out in microwave. In its conventional form, this kind of reaction needs a massive use of solvents and high temperature.[20] Indeed, a convenient alternative is precisely the use of microwave, that is known to promote faster reactions with small organic molecules, with very good yields.[21] The same approach has been applied also to bigger molecules obtaining great results.

In this project the most used reagent is 2,3,4,5-tetrakis(4-tert-butylphenyl)cyclopenta-2,4-dien-1-one, called simply ^{t}Bu-cyclopentadienone (compound **10**) (fig. 1.4).

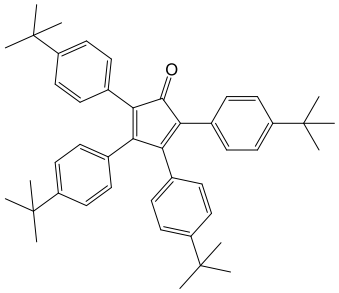

*Figure 1.4 – Compound **10***

The conditions used were the same for all the compounds and they were previously established by the group. As it is possible to see (fig. 1.5), the main idea was to use compound **10** both as reagent and solvent for the other reacting specie. The conditions chosen were optimal for the last elimination, too.

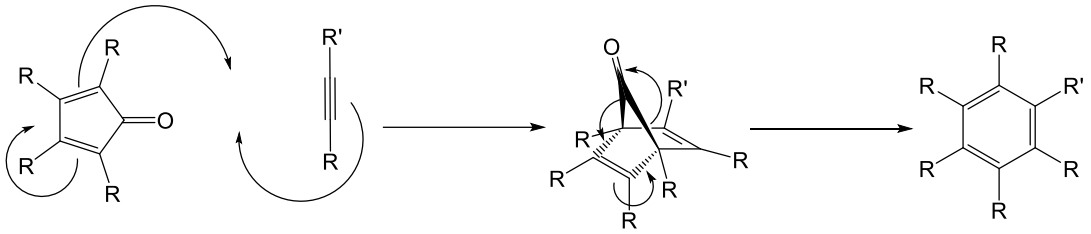

Figure 1.5 – Reaction mechanism scheme. The Diels – Alder reaction between a diene and a dienophile is followed by a reaction of elimination to obtain a more stable conjugated system

1.6.2 Suzuki – Miyaura coupling reaction

The Suzuki – Miyaura is a well-known and widely used rection, consisting in the coupling between two sp^2 carbon atoms (formerly bound to an halogen and to a boronic moiety respectively) promoted by a metal catalyst. More specifically, in this project we have used it for the coupling between two aromatic systems by means of a palladium catalyst.

The first step is the oxidative addition (fig. 1.6), where the palladium atom is oxidized donating electrons to make a new bond with a sp^2 carbon formerly bonded with a halogen. In the following step, called transmetalation, the organic group is transferred from the boronic ester to the palladium atom. Finally, a reductive elimination restores the metallic palladium and affords the target organic compound with a new C-C bond.[22]

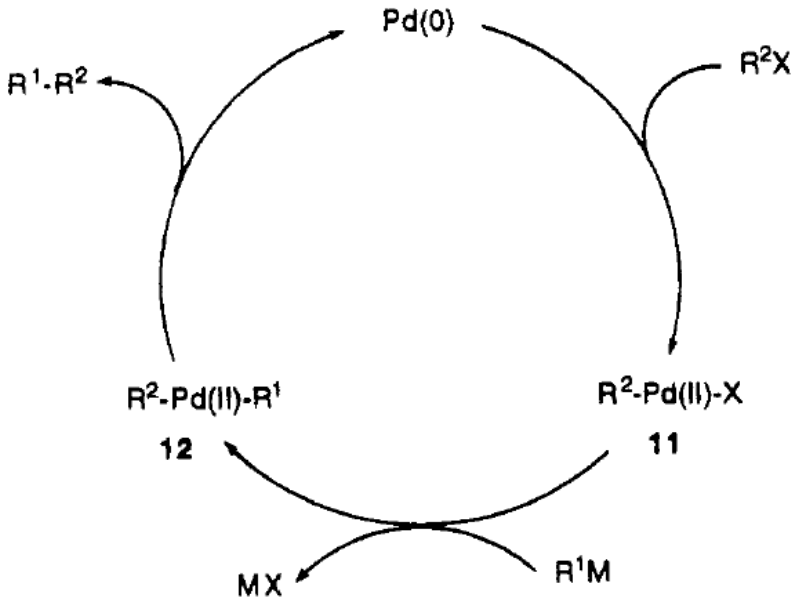

Figure 1.6 – Suzuki – Miyaura coupling reaction scheme[23]

As source of boron atoms, in this project it was used the so-called bis(pinacolato)diboron, a covalent compound containing two boron atoms and two pinacolato ligands (fig. 1.7).

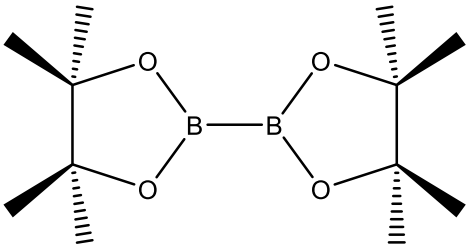

Figure 1.7 – Bis(pinacolato)diboron

Pinacol boronic esters are a class of new boron reagents that, despite being quite better than the old classes, like alkenylborones, are considered one of the less reactive due to the low nucleophilicity; even less reactive than their respective acid because the lone pairs of the oxygen atoms are conjugated into the electron deficient boronic centre through the σ-donating ability of carbon atoms.

The ester form was chosen because it readily dissolves in apolar solvents and it is not hydrogen bond donor, thus preventing oligomerization.

It is important to keep in mind that the boronic ester are still enough reactive for our aim and they are less costly.[22]

As bases, in this project both sodium (pK_a = 10.33) and potassium carbonate (pK_a = 10.25) were used, which can help the selective coupling of organoboron compounds with organic.[23]

1.6.3 Scholl reaction

The Scholl reaction is an acid catalysed oxidative condensation of aryl groups involving the formation of new C-C covalent bonds.[24] It is therefore an important tool to synthetise large π-extended systems such as nanographenes and heterocyclic analogues. The reaction can be both inter- and intramolecular: the latter being entropically preferred, and the only one used in this study.

Although being a very effective synthetic tool, this reaction present an impactful problem: indeed it is still a not well established reaction, lacking of a deep knowledge about the mechanism that rules it. It is known that the mechanism depends on the reagents used, and two main paths have been theorised: one through an arenium cation and one through radical cation (fig. 1.8).

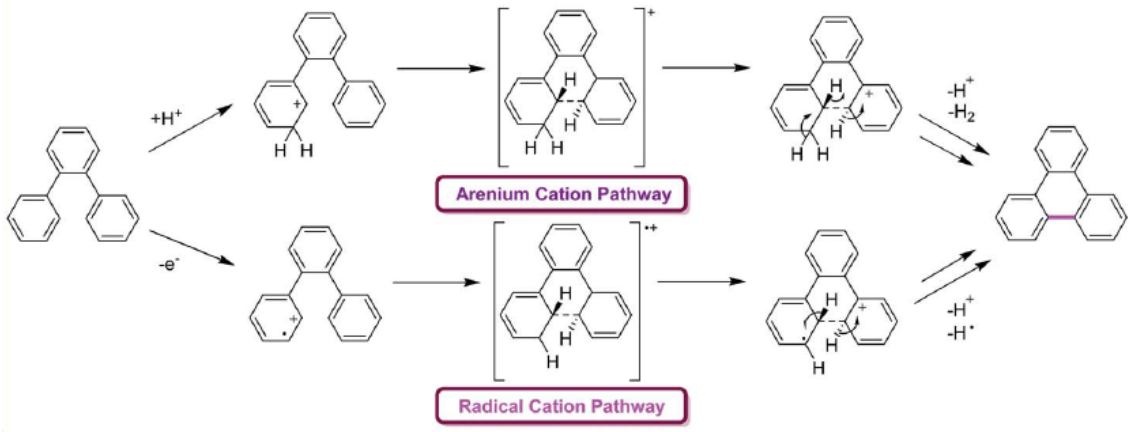

Figure 1.8 – Proposed mechanisms for the Scholl reaction[24]

At this point, it is worth introducing some reagents for the Scholl reaction, above all the ones used in this project.

The aluminium (III) chloride ($AlCl_3$) is the most used reagent and also the first one used by Scholl and Mansfeld.[25] Very often, it is used with $CuCl_2$ to improve the yield.

Later, it was seen that the synergic use of chlorobenzene and $AlCl_3$ was a good combination. Chlorobenzene is used as mild oxidant and $AlCl_3$ as non-oxidizing Lewis acid, implying that the oxidation is operated mainly by air at high temperatures.

Iron (III) chloride ($FeCl_3$) is used both as oxidizing agent and as Lewis acid, mainly because it is easy to find and ecofriendly. In synergy, chlorinated solvents gave faster reactions than CH_3NO_2 or hexane.[26]

The DDQ (2,3-Dichloro-5,6-dicyano-1,4-benzoquinone) – acid system is a very good agent to oxidise aromatic donors with a very high oxidation potential (~1.7 V, very strong oxidizing agent) to the corresponding cation radical.
More specifically, DDQ in combination with trifluoromethanesulfonic acid (CF_3SO_3H) is used for reactions of electron poor polyphenylenes with electron withdrawing groups such as -Br and -F. The protic acid has an important role in the progress of the reaction.[27]

1.7 Aggregation-induced emission

Luminescence has been studied for long time and generally experiment on organic molecules have been carried on in solution state. Very soon, it has been seen that many organic luminophores show different behaviour in diluted or concentrated solution, moreover luminescence is often weakened or even quenched at high concentrations: nowadays, it is a well-known phenomenon called concentration quenching. The main cause of this phenomenon is connected to a formation of aggregates in solution.
Later, it has been discovered a similar but opposite phenomenon where the luminescence is improved with the aggregation. So, it is possible to obtain a very strong luminescence from a solution highly concentrated or even from a solid film. This phenomenon is called aggregation-induced emission (AIE).
It has been studied a possible cause of it. In fact, in the aggregate state, the studied molecules cannot π-π stack due to its helix shape and the intramolecular rotations are greatly restricted avoiding non-radiative phenomena which could compete with radiative phenomena.
The result is that it is possible to obtain highly luminescent solutions by acting on proportions between solvents with the aim to decrease solubility and induce aggregation of the organic molecules.[28]

1.8 Purpose of the thesis

This project of thesis has been designed to investigate on the synthesis of three organic molecules belonging to the nanographenes with the future purpose of preparing functional materials for applications in fields such as photovoltaics.

Synthesis is followed by the characterization of these molecules using techniques such as ^{1}H and ^{13}C-NMR, mass spectrometry, optical absorbance and emission, concluding with electrochemistry experiments. In this way it has been possible to provide a well-rounded description of the new obtained molecules.

Finally, it has been investigated how optical emission of the products is affected by aggregation in solution, opening appealing opportunities for technological applications.

2 Experimental Part

2.1 Solvents, reagents and starting materials

Commercial solvents and reagents are reported in the tables below. Solvents and reagents were used without any further purification, unless specified.

Solvent	MW (g/mol)	CAS Number
1,2-Dichloroethane anhydrous, 99.8%	98.96	107-06-2
DMAP, ≥99%	122.17	1122-58-3
Chloroform, ≥99.5%	119.38	67-66-3
DCM, ≥99.8%	84.93	75-09-2
EtOH	46.07	64-17-5
Ethyl acetate, ≥99.5%	88.11	141-78-6
MeOH, ≥99.8%	32.04	67-56-1
n-Hexane, ≥95%	86.18	110-54-3
n-Pentane anhydrous, ≥99%	72.15	109-66-0
DMF, ≥99.8%	73.09	68-12-2
DCC	206.33	538-75-0
Nitromethane, ≥95%	61.04	75-52-5
THF anhydrous, 250 ppm BHT as inhibitor, ≥99.9%	72.11	109-99-9
Toluene anhydrous, 99.8%	92.14	108-88-3
Triethylamine, ≥99.5%	101.19	121-44-8

NMR Solvent	MW (g/mol)	CAS Number
Deuterated chloroform, 99.8 atom % D	120.38	856-49-6

Catalyst	MW (g/mol)	CAS Number
$PdCl_2$(dppf)	731.70	72287-26-4
$PdCl_2(PPh_3)_2$, 98%	701.90	13965-03-2
$Pd(PPh_3)_4$, 99%	1155.56	14221-01-3

Reagent	MW (g/mol)	CAS Number
Acetic acid glacial, ≥99.7%	60.05	64-19-7
Aluminium chloride, 99%	133.34	7446-70-0
Bis(pinacolato)diboron, 99%	253.94	73183-34-3
Chromium(VI) oxide, ≥98%	99.99	1333-82-0
Copper(I) iodide, 98%	190.45	7681-65-4
Copper(II) acetate, 98%	181.63	142-71-2
DBU	152.24	6674-22-2
Iron(III) chloride, 97%	162.20	7705-08-0
Hydrochloric acid, 37%	36.46	7647-01-0
n-Butyllithium, 2.5 M in hexanes	64.06	109-72-8
Potassium acetate, ≥99%	98.14	127-08-2
Potassium carbonate, ≥99%	138.21	584-08-7
Potassium cyanide, ≥96%	65.12	151-50-8
Potassium hydroxide, 90%	56.11	1310-58-3
Sodium carbonate powder, ≥99.5%	105.99	497-19-8
TMSA, 98%	98.22	1066-54-2

2.2 Instruments and analytical procedures

2.2.1 NMR Spectroscopy

^{1}H and ^{13}C-NMR spectra were acquired in a Bruker Advance 300 (^{1}H: 400 MHz; ^{13}C: 101 MHz) spectrometer at 298 K

Chemical displacements are expressed in part per million (ppm) referencing the solvent. The data are expressed in the following order: chemical displacement, multiplicity (s=singlet, d=doublet, dd=double doublet, t=triplet, m=multiplet), coupling constants (Hz) and integration area.

2.2.2 Mass spectrometry

Mass spectra Matrix assisted Laser desorption ionization (coupled to a Time-of-Flight analyser) experiments (MALDI-TOF) were recorded on a MAT 95 thermo spectrometer and a Bruker REFLEX spectrometer respectively.

2.2.3 UV-Vis Spectroscopy

UV-Vis spectra were recorded in a Varian Cary 50 spectrophotometer.

2.2.4 Microwave oven

For the microwave reactions a Monowave 300 of Anton Paar was used.

2.2.5 Cyclic Voltammetry

Cyclic voltammetry (CV) experiments were conducted in 0.1 M solutions of NBu_4PF_6 in DCM. A glassy carbon electrode was used as working electrode, and platinum wires were used as counter and reference electrodes. Before each measurement, the solution was deoxygenated with N_2. Ferrocene was added as an internal standard; its oxidation potential in DCM was positioned at 0.634 V vs. NHE and HTMs' oxidation potential were recalculated in reference to NHE.

2.3 Synthesis and characterization

2.3.1 Synthesis of Compound 1

2.3.1.1 Synthesis of compound 4[29]

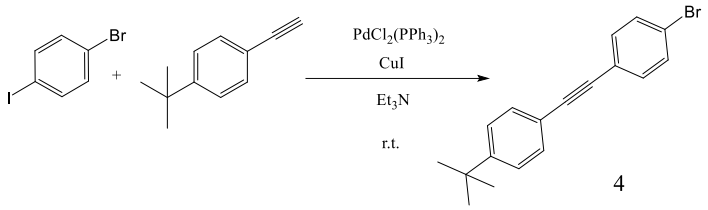

1-bromo-4-idobenzene (2.007 g, 7.09 mmol) was dissolved in triethylamine (35 mL) keeping the environment anhydrous.

After twenty minutes, $PdCl_2(PPh_3)_2$ (0.253 g, 0.036 mmol) and CuI (0.104 g, 0.546 mmol) were added. Then, 1-tert-butyl-4-ethynylbenzene (1.36 mL) was added at the solution. Then, it was let react for four hours.

The precipitate residue was filtered with a Buchner using hexane to wash the solid. The residue was purified by flash chromatography using hexane as eluent, yielding 2.018 g (6.44 mmol, yield of 91%) of compound **4**. The product showed identical spectroscopic properties to those reported in the bibliography.

^{1}H NMR (see Appendix).

2.3.1.2 Synthesis of compound 5[30]

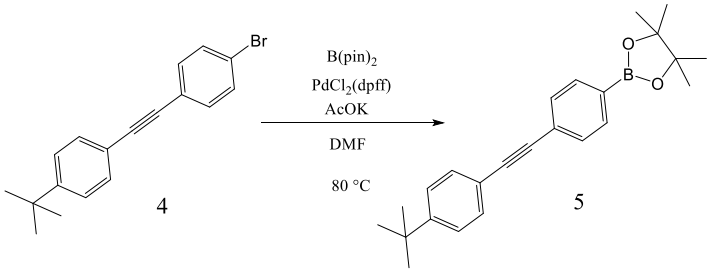

Anhydrous DMF (30 mL) and compound **4** (1.993 g, 6.36 mmol) were placed in a reaction flask. Then, bis(pinacolato)diboron (1.995 g, 7.86 mmol) and $PdCl_2$(dppf) (0.265 g, 0.36 mmol) were added. After fifteen minutes, potassium acetate (1.90 g, 19.3 mmol) was added. The reaction was let go for the whole night at 80 °C, obtaining a dark green solid.

A separation was performed with a separation funnel using DCM and HCl 10%. Then, the residue was purified by flash chromatographic using a mixture of hexane and DCM (1:1) yielding 1.679 g (4.66 mmol, yield of 73%) of compound

5. The product showed identical spectroscopic properties to those reported in the bibliography.

^{1}H NMR (see Appendix).

2.3.1.3 Synthesis of compound 6

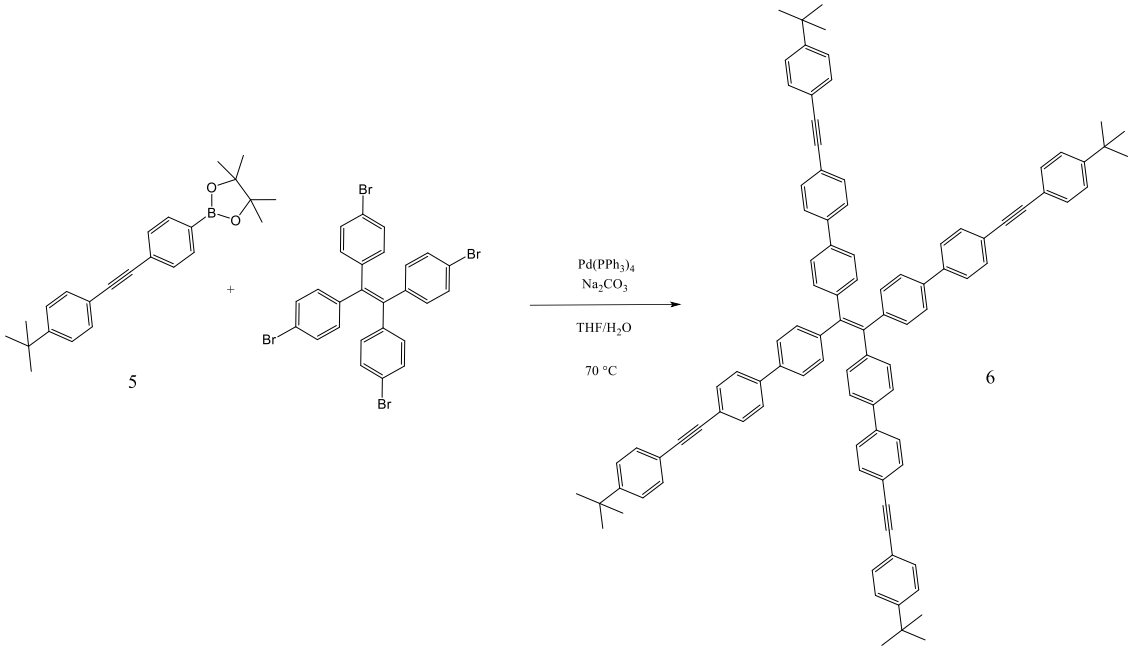

1,1,2,2-tetrakis(4-bromophenyl)ethylene (0.399 g, 0.62 mmol), compound **5** (1.008 g, 2.80 mmol) and sodium carbonate (0.392 g, 3.70 mmol) were dissolved in a mixture of THF (40 mL) and water (10 mL). Then, $Pd(PPh_3)_4$ (0.646 g, 0.56 mmol) was added to the mixture and the reaction was heated at 70 ºC for twenty four hours.

Then, the yellow precipitate was filtered using a Buchner and the solid was washed with chloroform. The solid (0.420 g, 0.33 mmol, yield of 53%) was collected without further purification.

^{1}H NMR (400 MHz, $CDCl_3$): δ (ppm) 7.70-7.15 (m, 48H), 1.25 (s, 36H). Mass analysis (MALDI-TOF) calculated (formula) 1260.66; experimental 1261.79.

2.3.1.4 Synthesis of compound 9[31]

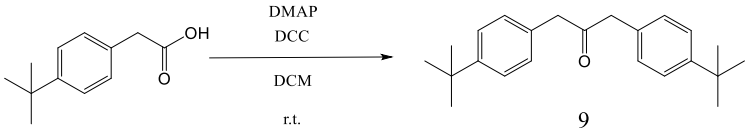

DMAP (0.518 g, 2.69 mmol) and DCC (3.293 g) were dissolved in of CH_2Cl_2 (25 mL). At the same time, 4-tert-butylphenylacetic acid (3.014 g, 15.7 mmol) were dissolved in CH_2Cl_2 (35 mL). At this point, the first solution was poured dropwise in the second one. As result, a yellow coloured solution was formed and it was let react for twenty four hours.

The residue of the reaction was filtered and washed with CH_2Cl_2. The orange/yellow coloured solution was dried in rotavapor obtaining a yellow coloured solid.

The residue was purified by flash chromatography using a mixture of hexane and ethyl acetate (10:1) as eluent yielding 1.032 g (3.20 mmol, yield of 41%) of compound **9**. The product showed identical spectroscopic properties to those reported in the bibliography. ^{1}H NMR (see Appendix).

2.3.1.5 Synthesis of compound 7[32]

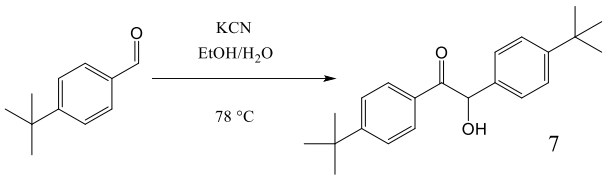

4-(tert-butyl)benzaldehyde (5.14 mL, 30.7 mmol) was dissolved in a mixture of ethanol (30 mL) and water (15 mL) and then KCN (0.403 g, 6.19 mmol) was added. The reaction was let go all night long at 78 °C.

After that, water was poured into the system enhancing the precipitation of the product. The solid was filtered with a Buchner funnel.

The compound **7** was a white solid and the mass obtained was 5.619 g (17.3 mmol, yield of 112%). The product showed identical spectroscopic properties to those reported in the bibliography. ^{1}H NMR (see Appendix).

2.3.1.6 Synthesis of compound 8[33]

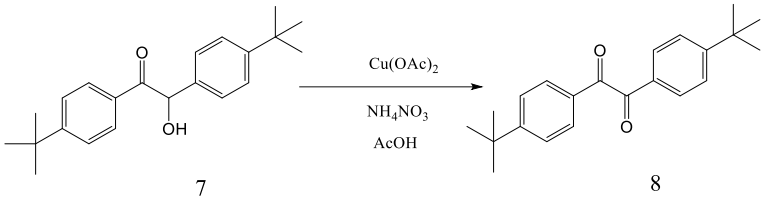

7 8

Compound **7** (5.605 g, 17.3 mmol), copper(II) acetate (6.984 g, 38.5 mmol) and nitromethane (0.632 g, 7.90 mmol) and acetic acid (20 mL) were joined together. The reaction was let go all night long at 100 °C.

The obtained mixture was separated with a separation funnel. Then, the residue was purified with a flash chromatography using DCM as eluent yielding 2.439 g (7.56 mmol, yield of 44%) of compound **8**. The product showed identical spectroscopic properties to those reported in the bibliography. ^{1}H NMR (see Appendix).

2.3.1.7 Synthesis of compound 10[34]

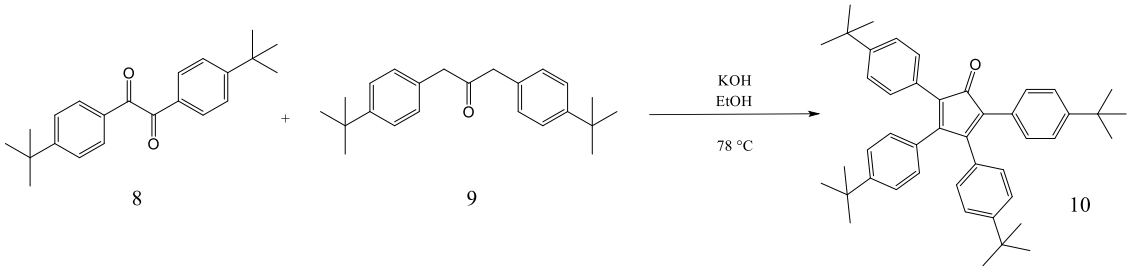

8 9 10

Compound **8** (4.0293 g, 12.5 mmol) and compound **9** (4.0488 g, 12.6 mmol) were dissolved in of ethanol (25 mL) and then the heating was brought at 78 °C. When everything was dissolved, KOH (0.8814 g, 15.7 mmol) was added and then the reaction was let go for two hours.

The product of the reaction was worked up and successively the residue was purified with flash chromatography using a mixture of hexane and DCM (6:1) as eluent yielding 1.684 g (2.77 mmol, yield of 22%) of compound **10**. The product showed identical spectroscopic properties to those reported in the bibliography. ^{1}H NMR (see Appendix).

2.3.1.8 Synthesis of compound 11

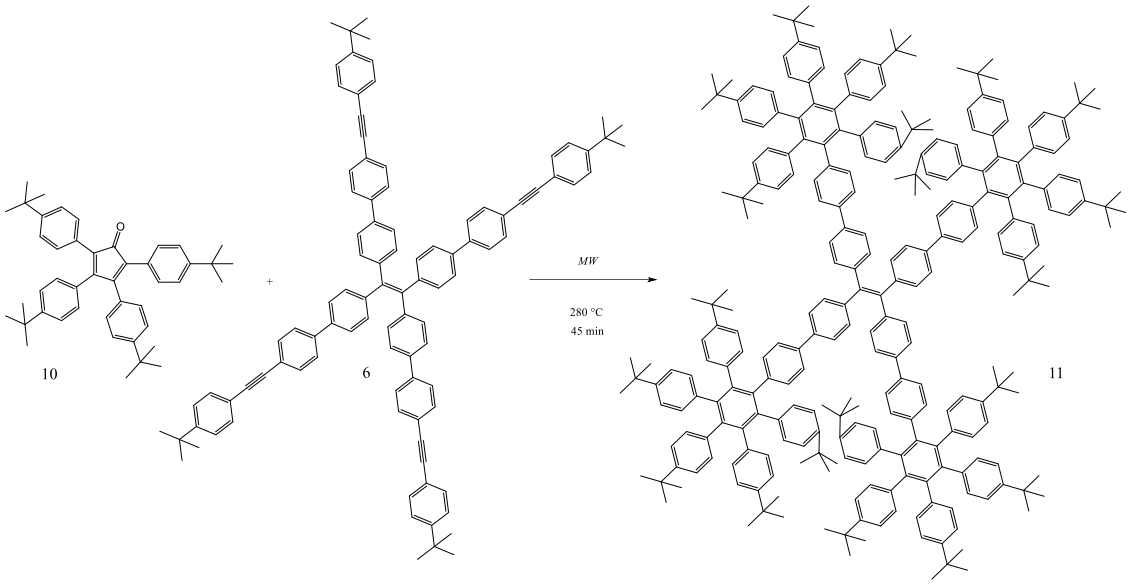

In a vial for microwave oven, compound **6** (0.1003 g, 0.080 mmol) and compound **10** (0.2447 g, 0.40 mmol) were joined together. The reaction was let go in the oven for forty five minutes at 280 °C. Then, the residue was purified by flash chromatography with a mixture of hexane and DCM (4:1) as eluent, yielding 0.285 g (0.079 mmol, yield of 99%) of compound **11**.

^{1}H NMR (400 MHz, $CDCl_3$): δ (ppm) 7.13 (m, 9H), 6.99 (m, 16H), 6.82 (m, 47H), 6.69 (m, 40H), 1.10 (s, 180H). Mass analysis (MALDI-TOF) calculated (formula) 3582.28; experimental 3585.43.

2.3.1.9 Synthesis of compound 1

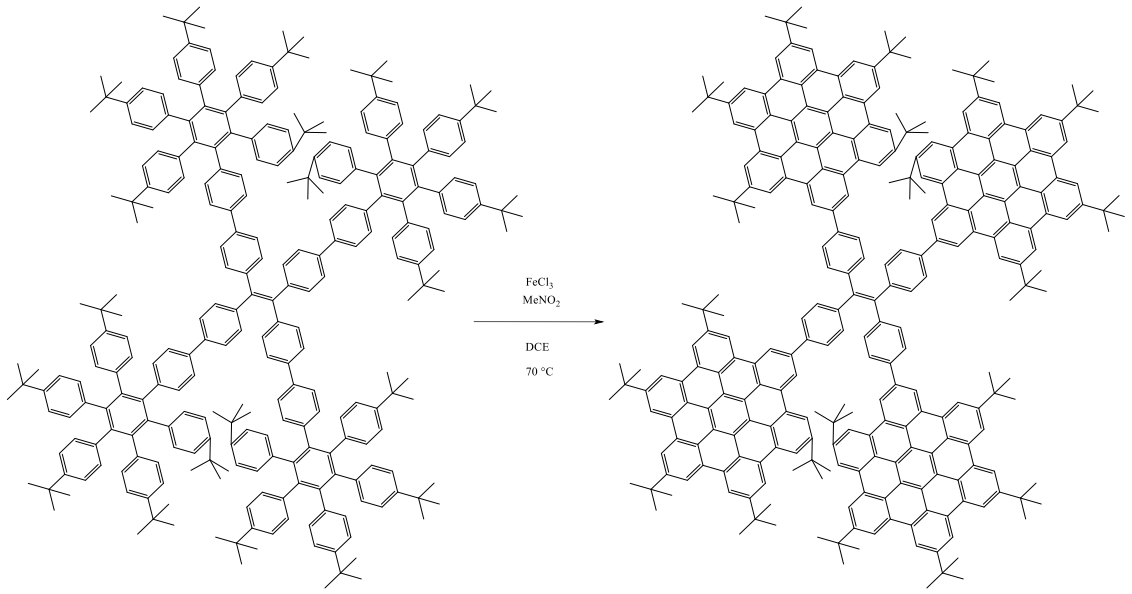

Compound **11** (0.285 g, 0.079 mmol) was dissolved in DCE (25 mL). Then, a second solution with $FeCl_3$ (1.2893 g, 7.95 mmol) and CH_3NO_2 (3 mL) was prepared and it was added to the first solution. The resulting mixture was heated at 70 °C for two hours.

The residue was purified by flash chromatography with a mixture of DCM and hexane (1:2) as eluent, yielding compound **1**.

^{1}H NMR (400 MHz, $CDCl_3$): n/a. ^{13}C NMR (101 MHz, $CDCl_3$): δ (ppm) 77.38, 77.35, 77.06, 77.03, 76.71, 32.10, 29.77. Mass analysis (MALDI-TOF) calculated (formula) 3533.91; experimental 3534.03.

2.3.2 Synthesis of Compound 2

2.3.2.1 Synthesis of compound 12[35]

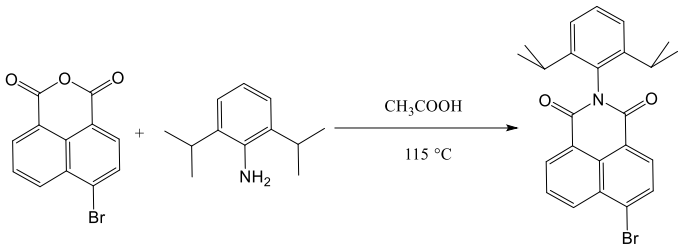

12

4-bromo-1,8-naphthalic anhydride (2.013 g, 7.26 mmol) and of acetic acid (50 mL) were joined together. Then 2,6-diisopropylaniline (4.10 mL) was added. The reaction was maintained refluxing (T = 115 °C) and let it react all night long.

The resulting precipitate was filtered with a Buchner funnel and washed it with water obtaining 2.370 g (5.43 mmol, yield of 75%) of compound **12**. The product showed identical spectroscopic properties to those reported in the bibliography.

^{1}H NMR (see Appendix).

2.3.2.2 Synthesis of compound 13[36]

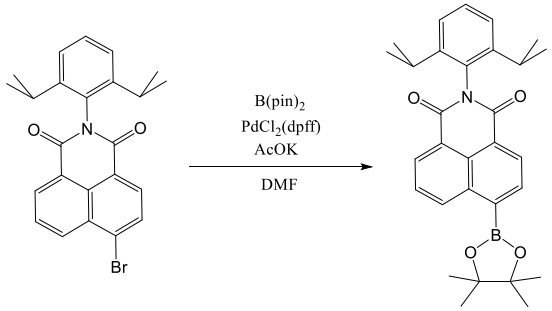

12 13

Compound 12 (2.370 g, 5.43 mmol) was dissolved in anhydrous DMF (30 mL). Then, bis(pinacolato)diboron (1.656 g, 6.52 mmol) and $PdCl_2$(dppf) (0.223 g, 0.30 mmol) were added. After fifteen minutes, potassium acetate (1.602 g, 16.3 mmol) was added. The reaction was let go for the whole night at 80 °C.

The residue was purified by flash chromatography using DCM as eluent obtaining 0.239 g (0.49 mmol, yield of 9%) of compound **13**. The product showed identical spectroscopic properties to those reported in the bibliography.

^{1}H NMR (see Appendix).

2.3.2.3 Synthesis of compound 14

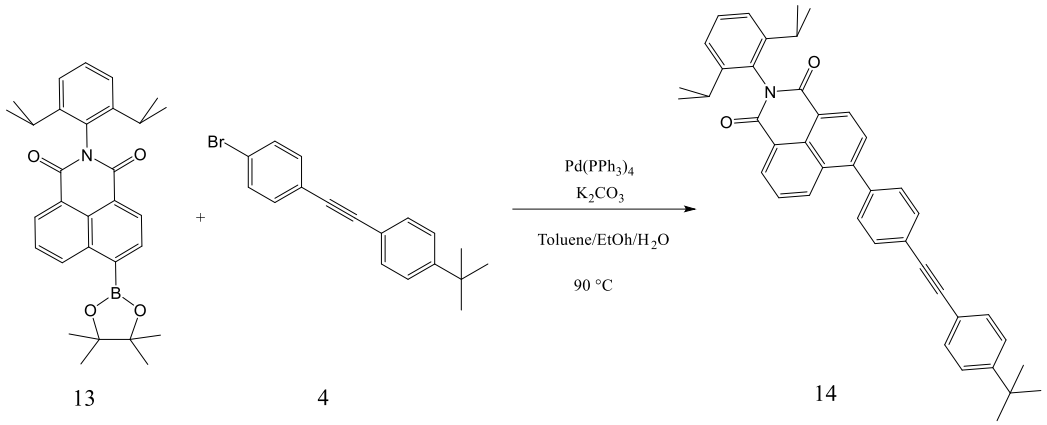

Compound **13** (0.927 g, 1.92 mmol), compound **4** (0.602 g, 1.92 mmol) and K_2CO_3 (0.800 g, 5.79 mmol) were dissolved in 30 mL of a mixture of THF, ethanol and water (4:1:1) minding to keep an anhydrous environment. After that, $Pd(PPh_3)_4$ (0.114 g, 0.098 mmol) was added. It was let react for twenty four hours at 90 °C.

The residue was purified by flash chromatography with a mixture of DCM and hexane (1:1) as eluent, yielding 0.873 g (1.48 mmol, yield of 77%) of compound **14**.

^{1}H NMR (400 MHz, $CDCl_3$): δ (ppm) 8.75-7.2 (m, 16H), 1.55-1.15 (m, 21H). Mass analysis (MALDI-TOF) calculated (formula) 589.30.

2.3.2.4 Synthesis of compound 15

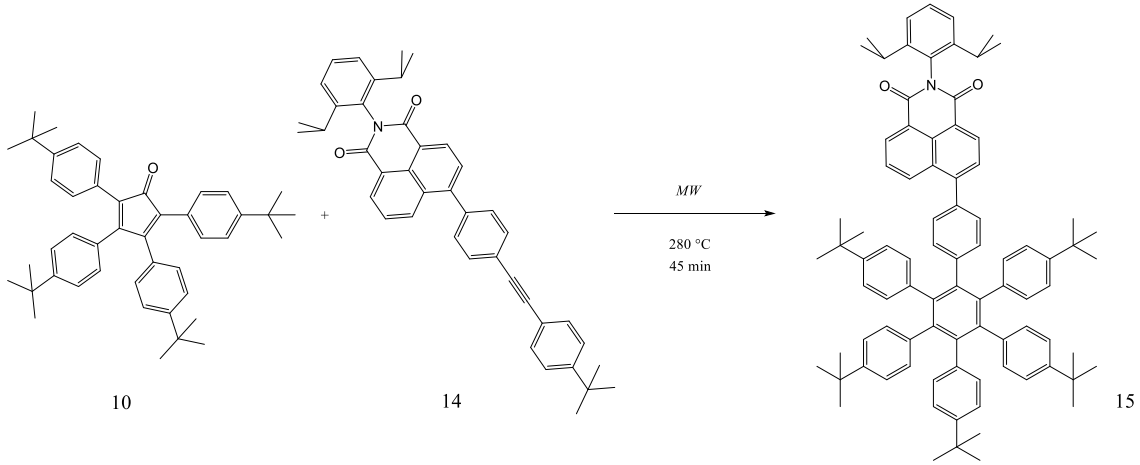

10 14 15

In a vial for microwave oven, compound **14** (0.204 g, 0.35 mmol) and compound **10** (0.253 g, 0.41 mmol) were joined together. The reaction was let reacting in the oven for forty five minutes at a temperature of 280 °C. Then, the residue was purified by flash chromatography with a mixture of hexane and DCM (1:1) as eluent, yielding 0.394 g (0.34 mmol, yield of 97%) of compound **15**.

^{1}H NMR (400 MHz, $CDCl_3$): δ (ppm) 8.61 (dd, J = 9.2, 7.4 Hz, 2H), 7.93 (d, J = 8.6 Hz, 2H), 7.62-7.55 (m, 2H), 7.46 (dd, J = 10.1, 7.6 Hz, 2H), 7.32 (d, J = 7.7 Hz, 2H), 7.01 (q, J = 8.3 Hz, 2H), 6.93 (d, J = 8.4 Hz, 2H), 6.87-6.78 (m, 4H), 6.72 (d, J = 8.4 Hz, 2H), 2.77-2.68 (m, 1H), 1.53-1.0 (s, 57). Mass analysis (MALDI-TOF) calculated (formula) 1169.71; experimental 1170.74.

2.3.2.5 Synthesis of compound 2

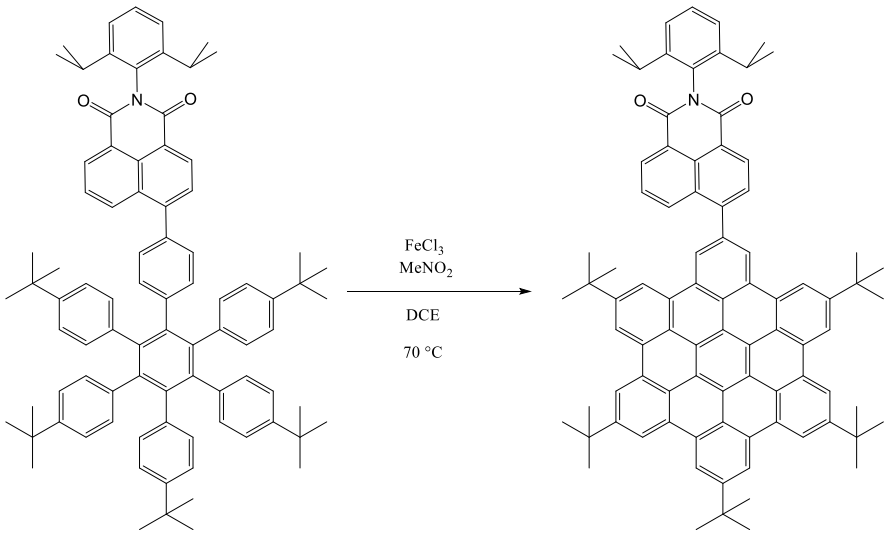

15 2

Compound **15** (0.201 g, 0.17 mmol) was dissolved in DCE (25 mL). After that, $FeCl_3$ (0.7223 g, 4.45 mmol) was dissolved in CH_3NO_2 (2 mL) and then was added at the first solution. The final mixture was heated at 70 °C for two hours. To purify the residue, a flash chromatography was made with a mixture of hexane and DCM (1:1), yielding 0.132 g (0.114 mmol, yield of 67%) of compound **2**.

^{1}H NMR (400 MHz, $CDCl_3$): δ (ppm) 9.37-9.30 (m, 1H), 9.22 (s, 1H), 9.02 (d, J = 7.4 Hz, 1H), 8.84 (d, J = 7.2 Hz, 1H), 8.64 (d, J = 8.6 Hz, 1H), 8.30 (d, J = 7.4 Hz, 1H), 7.86 (dd, J = 8.4, 7.3 Hz, 1H), 7.58-7.52 (m, 1H), 7.42 (d, J = 7.7 Hz, 1H), 2.98-2.86 (m, 1H), 1.85-1.0 (s, 57H). ^{13}C NMR (101 MHz, $CDCl_3$): δ (ppm) 164.45, 164.27, 149.36, 149.28, 148.17, 145.77, 136.72, 133.38, 131.97, 131.49, 131.22, 130.96, 130.61, 130.35, 129.77, 129.54, 128.76, 124.06, 121.12, 119.93, 119.18, 119.04, 77.35, 77.04, 76.72, 35.79, 32.03, 29.27, 24.11. Mass analysis (MALDI-TOF) calculated (formula) 1157.61; experimental 1158.61.

2.3.3 Synthesis of Compound 3

2.3.3.1 Synthesis of compound 16

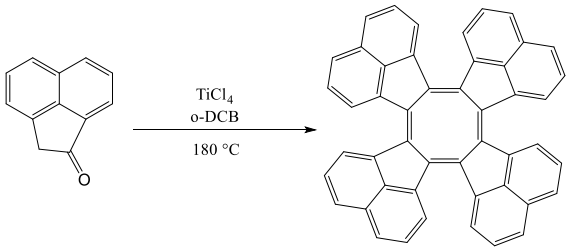

16

$TiCl_4$ (10.30 mL, 93 mmol) was dissolved in o-DCB (50 mL) in anhydrous environment. After that, acenaphthylene-1(2H)-one (2.63 g, 15.6 mmol) was dissolved in o-DCB (25 mL) and then the solution was added in the first one. The resulting mixture was let react for three hours at a temperature of 180 °C.

After that, the mixture was poured in a flask with HCl concentrated and ice.

The residue was purified by flash chromatography with a mixture of hexane and DCM (3:1), yielding compound **16**.

^{1}H NMR (400 MHz, $CDCl_3$): δ (ppm) 7.87 (d, J = 8.1 Hz, 2H), 7.68 (d, J = 6.9 Hz, 2H), 7.57 (dd, J = 8.0, 7.1 Hz, 2H). Mass analysis (MALDI-TOF) calculated (formula) 600.19.

2.3.3.2 Synthesis of compound 17

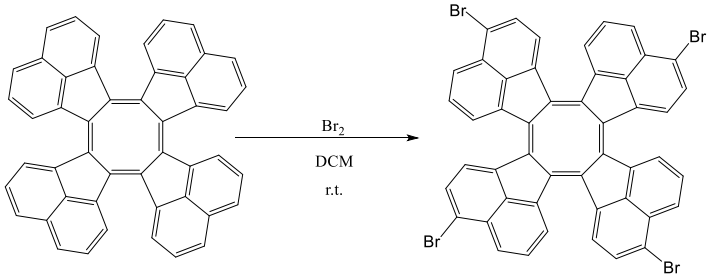

16 17

Compound **16** (0.256 g, 0.43 mmol) and Br_2 (0.0874 mL, 1.71 mmol) were dissolved in DCM (10 mL). The mixture was let react for forty eight hours at room temperature.

The residue was purified by flash chromatography using a mixture of hexane and DCM (3:1), yielding 0.318 g (0.35 mmol, yield of 81%) of compound **17**.

^{1}H NMR (400 MHz, $CDCl_3$): δ (ppm) 8.05-8.00 (m, 1H), 7.75 (dd, J = 7.4, 1.6 Hz, 1H), 7.65-7.59 (m, 2H), 7.41 (dd, J = 7.4, 1.4 Hz, 1H). Mass analysis (MALDI-TOF) calculated (formula) 911.83.

2.3.3.3 Synthesis of compound 3’

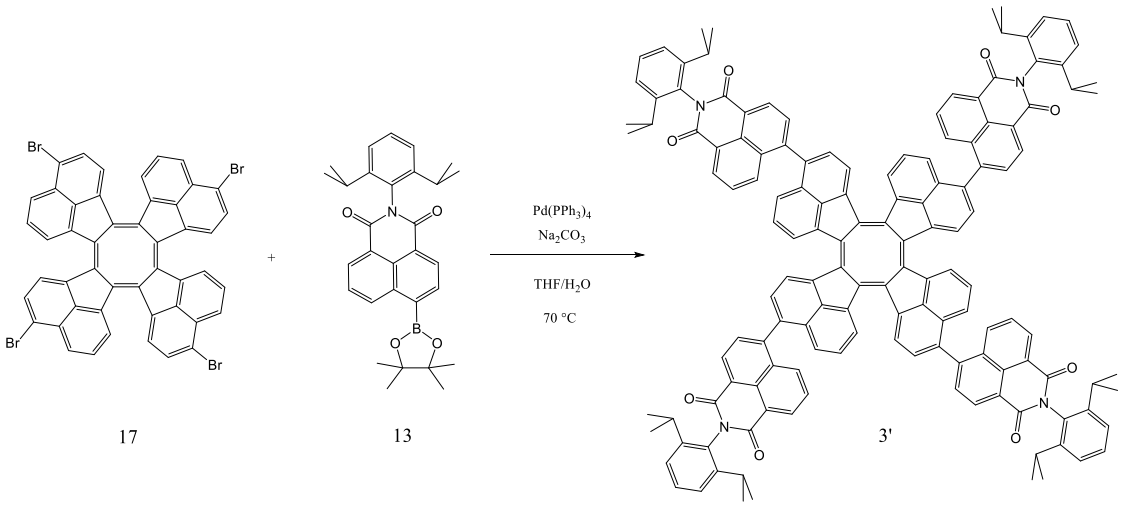

17 13 3'

Compound **17** (0.318 g, 0.35 mmol), compound **13** (0.760 g, 1.57 mmol), Na_2CO_3 (0.261 g, 2.47 mmol) were dissolved in 50 mL of a mixture of THF and water (4:1), in an anhydrous environment. After that, $Pd(PPh_3)_4$ (0.089 g, 0.08 mmol) was added. Then, the reaction was heated at 70 °C and it was let react for twenty four hours.

The residue was purified by flash chromatography using a mixture of DCM and hexane (4:1) as eluent, yielding 0.648 g (0.32 mmol, yield of 91%) of compound **3'**.

^{1}H NMR (400 MHz, $CDCl_3$): δ (ppm) 8.9-7.3 (m, 52H), 1.30-1.10 (m, 48H). ^{13}C NMR (101 MHz, $CDCl_3$): δ (ppm) 171.16, 164.23, 164.12, 164.07, 145.67, 144.33, 141.19, 140.76, 137.74, 133.41, 133.18, 131.89, 131.81, 131.73, 130.97, 130.80, 130.25, 129.14, 128.75, 125.68, 77.35, 77.03, 76.71, 60.41, 29.23, 24.03, 21.06, 14.21. Mass analysis (MALDI-TOF) calculated (formula) 2020.82; experimental 2021.94.

3 Results and Discussions

As it was already introduced, this thesis project had the purpose of finding the best synthetic route to afford specific organic molecules characterised by an extended π system and their characterization.

Talking about characterization, the techniques used are ^{1}H-NMR, ^{13}C-NMR, mass spectrometry, UV-Vis spectroscopy and circular voltammetry.

3.1 Synthesis

When a synthetic route is designed, quite often you must choose between some different possibilities. In the case of this project, it was very important not only reaching the target product but also doing it with the simplest conditions, thinking of a possible daily production in the future. This means that the smallest number of synthetic steps using very common and harmless reagents were needed. Keeping in mind this, and also the “green issues” when it was possible, a non-solvent path was preferred.

So, in this section the whole synthetic routes will be exposed (fig. 3.1, fig. 3.2, fig. 3.3).

Moreover, also the alternative route will also be shown and commented. The synthetic methodology that has been followed, together with the experimental details, is given in the experimental part.

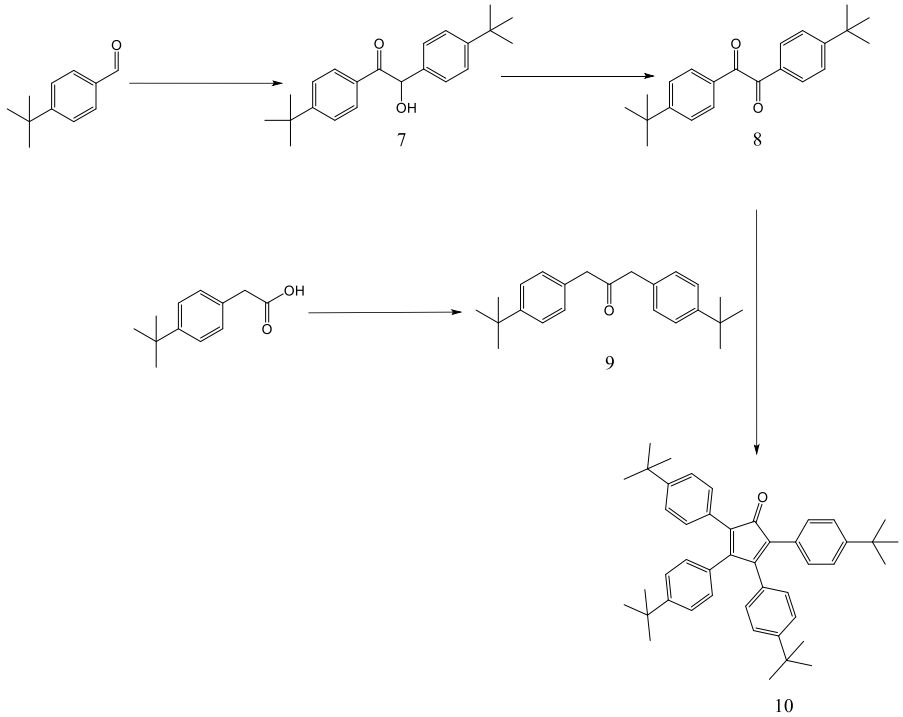

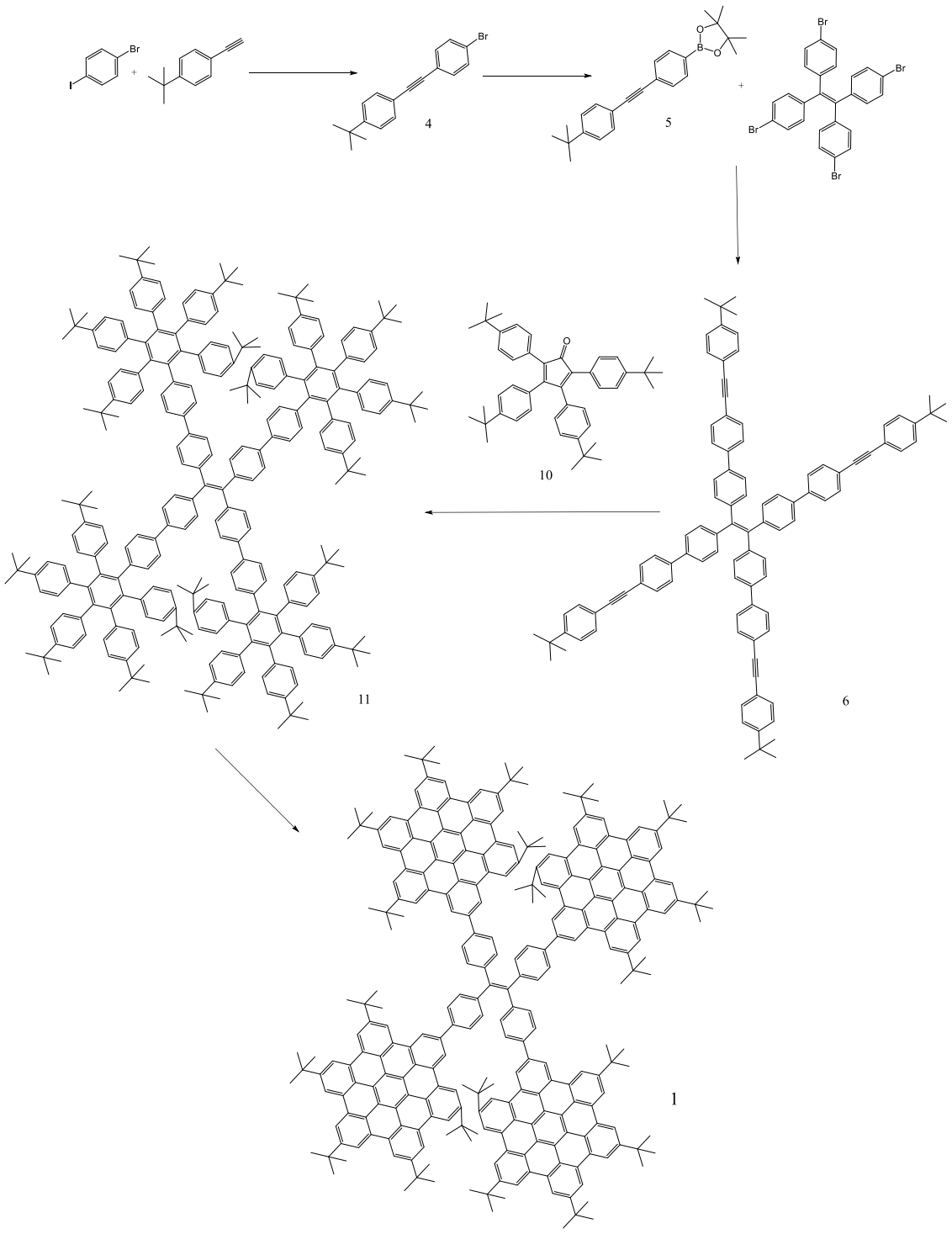

*Figure 3.1 – Synthetic rout towards compound **1***

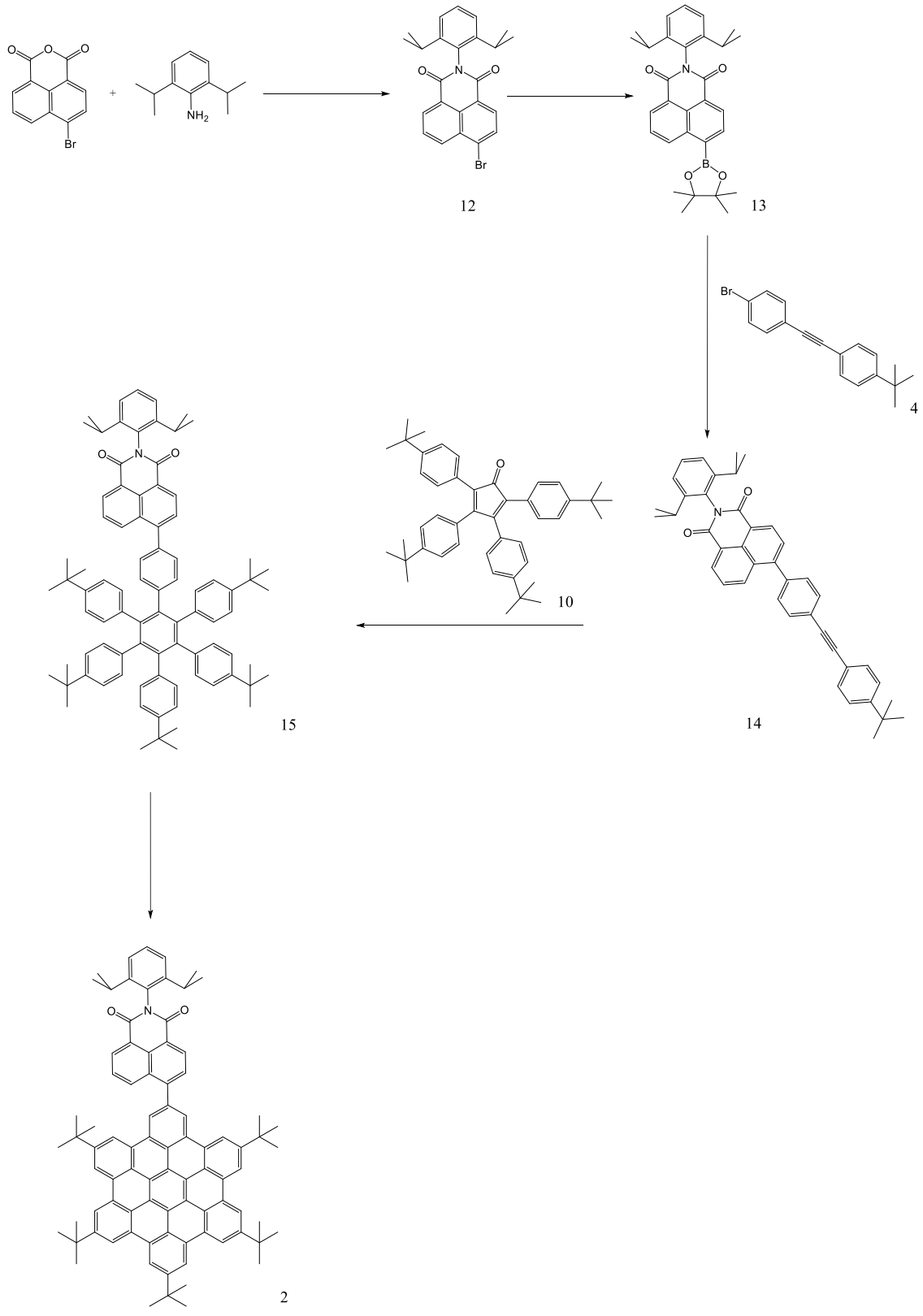

*Figure 3.2 – Synthetic rout towards compound **2***

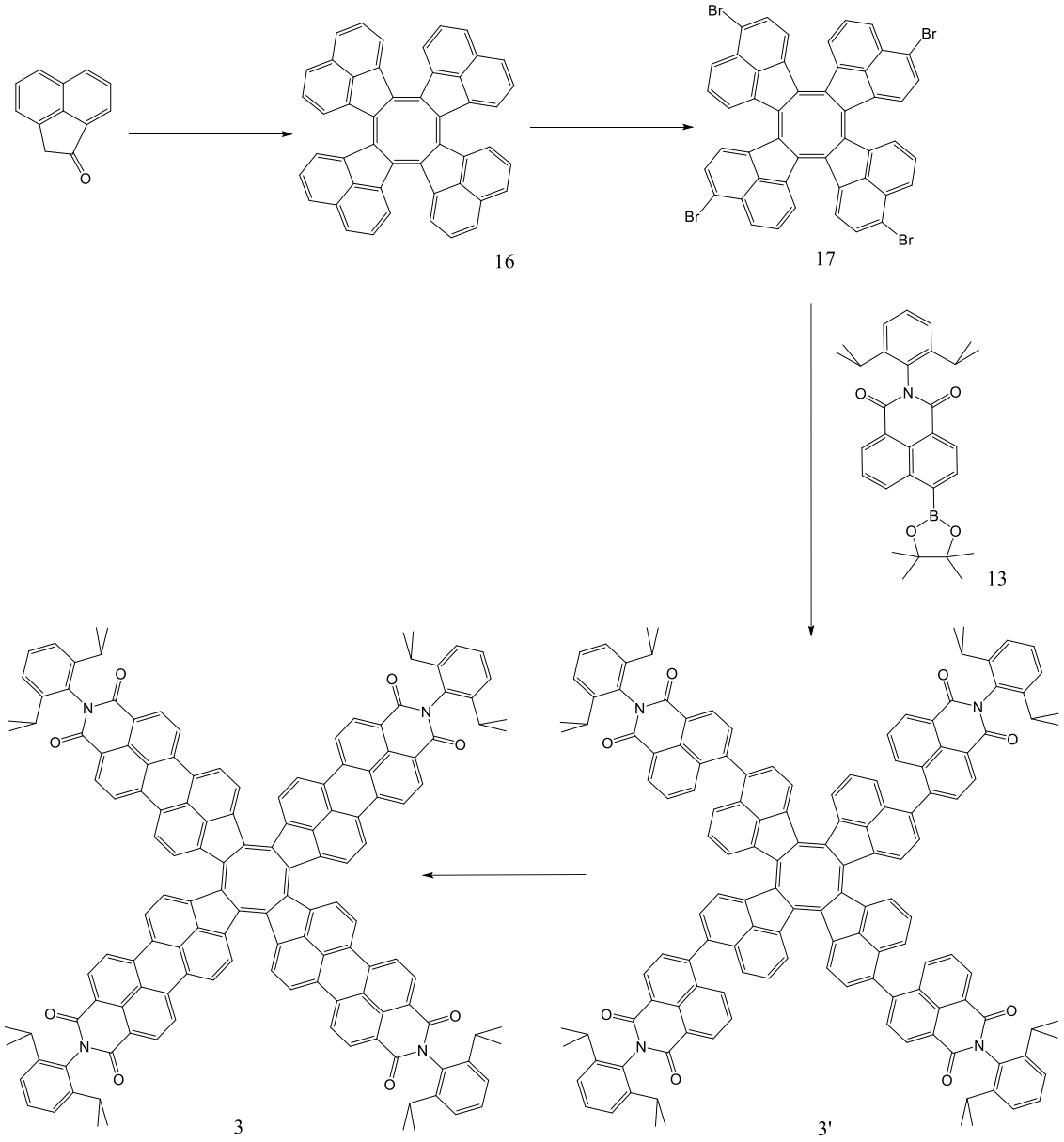

*Figure 3.3 – Synthetic rout towards compound **3***

3.1.1 Compound 1

The synthetic pathway towards target compound **1** started from 4-tert-butylphenylacetylene and 1-bromo-4-iodobenzene. In fact, the first step was the Sonogashira cross-coupling reaction between these two starting compounds with $PdCl_2(PPh_3)_2$ as catalyst. With this reaction it was possible to obtain the compound **4**. It is interesting how the reaction was carried out in the iodine site due to its reactivity, leaving the bromine site unreacted and ready for the next reaction.

As we will see later, this compound was then used in a Suzuki – Miyaura coupling reaction. The following step consisted of a palladium-catalysed substitution with bis(pinacolato)diboron at the unreacted bromine site to obtain the boronic ester (**5**) which would react in the following step with an halide compound. Here, 1,1,2,2-tetrakis(4-bromophenyl)ethylene was used (fig. 3.4).

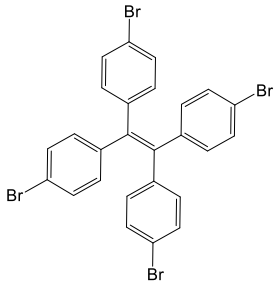

Figure 3.4 – 1,1,2,2-tetrakis(4-bromophenyl)ethylene

The desired compound **6** was successfully furnished by fourfold palladium-catalyzed Sonogashira cross-coupling using four times more equivalents of compound **5** than compound **1**. Compound **6** underwent a microwave-assisted [4 + 2] cycloaddition with 2,3,4,5-tetrakis[4-(1,1-dimethylethyl)phenyl]2,4-cyclopentadien-1-one (**10**) giving rise to **11**. This reaction is a Diels – Alder cycloaddition between the alkynes (as dienophiles) in compound **6** and the conjugated double bond in cis position of the central five-membered ring in compound **10**. This step is rapidly followed by a thermally induced elimination of the ketonic group to restore a larger conjugation in polycyclic aromatic hydrocarbon **11**. This approach is interesting because it is solventless.

On the other hand, 4-tert-butylbenzaldehyde was reacted firstly with KCN and subsequently with itself, giving compound **7** as a product, ready to be oxidised with copper(II) acetate in acetic acid to afford compound **8**. This one was reacted

with compound **9** in basic conditions to obtain the key product, tBu-cyclopentadienone (**10**) (fig. 1.4).
Stepping back, compound **9** was obtained from a condensation rection catalysed by DMAP and DCC of (4-tert-butylphenyl)acetic acid.
The final reaction is a cyclodehydrogenation, namely Scholl reaction, which permits to obtain an even higher conjugated molecule (**1**). Polycyclic aromatic hydrocarbon **11** was treated in the presence of $FeCl_3$ producing the corresponding molecular nanographene (**1**).

3.1.2 Compound 2

The synthetic pathway towards target compound **2** started from 6-bromo-1H,3H-benzo[de]isochromene-1,3-dione and 2,6-diisopropylaniline which were reacted in acidic environment to obtain the compound **12**, a molecule with an higher extended conjugation.
At this point, the bromine site was suitable for the Suzuki – Miyaura coupling reaction. The starting point is the substitution of the bromine atom with the boron ester, in the already seen conditions. Then, the boron ester (**13**) was reacted with compound **4** which present a reactive bromine site, obtaining compound **14**.
Then, compounds **14** and **10** were reacted in a microwave oven as previously seen, through a Diels – Alder cycloaddition and the following elimination to obtain compound **15**. This compound shows a hexa-substituted benzene ring as a central member and a high conjugation. This structure is a functionalized hexaphenylbenzene (HPB).
Then, through a reaction Scholl, the HPB structure was closed with the formation of new C-C bonds obtaining a functionalised hexa-peri-hexabenzocoronene (HBC).
HBC is a disc-shaped polycyclic aromatic hydrocarbons that can self-associate into columnar stacks through strong π–π interactions. By functionalising the HBC molecule, a range of properties and functions can be obtained such as solution processability and conductivity.[37]
However, the route shown was not the first attempt, in fact the first idea was slightly different.

Once obtained the compound **13**, it was designed to react with an HBC group with a mono bromine substituent through a Suzuki – Miyaura coupling reaction (fig. 3.5).

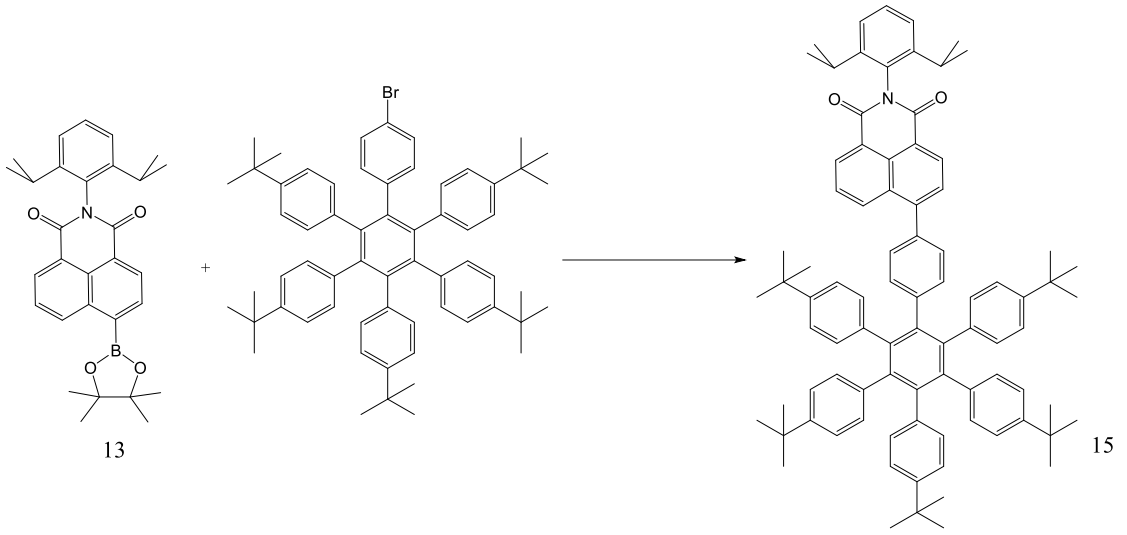

*Figure 3.5 – Alternative route for the synthesis of compound **15**. Here, compound **1** reacts with functionalised HPB*

This reaction was tried in two different conditions: both were carried out with $Pd(PPh_3)_4$ as catalyst, but using respectively Na_2CO_3 in THF/H_2O at 70 °C and K_2CO_3 in $Toluene/EtOH/H_2O$ at 90 °C. This last reaction afforded the product, but yield was lower than 40%.

3.1.3 Compound 3

The synthetic pathway towards target compound **3** started from 1-acenaphthenone. The reaction with $TiCl_4$ in o-DCB was used to tetramerise the reagent, obtaining a new compound (**16**) with a specific feature: an eight-membered central ring with four “branches” composed by the former acenaphthene group.

The following reaction is a bromination at room temperature. This one is somehow easy to carry on. In fact, at room temperature the bromination takes place just once for each acenaphthene group. This means that the resulting compound **17** was monosubstituted in each branch. A mixture of isomers was obtained depending on the position of bromine atoms, but it was not causing any problem in the following synthetic steps. This mixture of isomers is visible in ^1H NMR spectra.

At this point, compound **17** was reacted with compound **13** through a Suzuki – Miyaura coupling reaction. The equivalents of the second reagent were four times the ones of the first reagent to be sure that reaction could be carried out in all four reactive bromine sites. The resulting compound **3'** was in a mixture of all the possible isomers, too.

The reaction carried out to obtain the compound **3** was a Scholl reaction. Different conditions were tried but it was not possible to obtain the target product.

In a first attempt, $AlCl_3$ in o-dichlorobenzene was used. Since it did not work, $FeCl_3$ in nitromethane was tried. When neither this approach worked, it was decided to use as reagent DDQ in two different conditions, firstly in trifluoromethanesulfonic acid and subsequently in DCM.

Unfortunately, none of these reactions worked and a suitable route still has to be designed.

Before that, an alternative route was firstly tried (fig. x). While in the route just described, the eight-member central ring was synthesised first and then functionalised, in this second approach, the main idea was to synthesise the branches first and then condense them together to obtain the final compound (**3**).

More specifically, the synthetic route started with the reaction of bromination of acenaphthene by NBS obtaining a mono substituted compound (**16**). As explained before, the molecule was mono substituted thanks to the conditions of reaction. At this point, compound **13** (a boronic ester) and **16** (an halide) were reacted through a coupling reaction which permitted the formation of a new C-C bond between the two molecules, obtaining the compound **18** as product. This one was reacted through a Scholl reaction, with the purpose of closing the conjugation, forming a new bond between the two close, but unbound, benzene rings.

At this point, a reaction of oxidation was performed with the hope of oxidising the five-member ring of the former acenaphthene obtaining the compound **20**.

Unfortunately, what was obtained was a reddish solid which was found out not being the wanted compound thanks to the mass analysis spectrometry. It has been decide to newly carry out this route in the future PhD project.

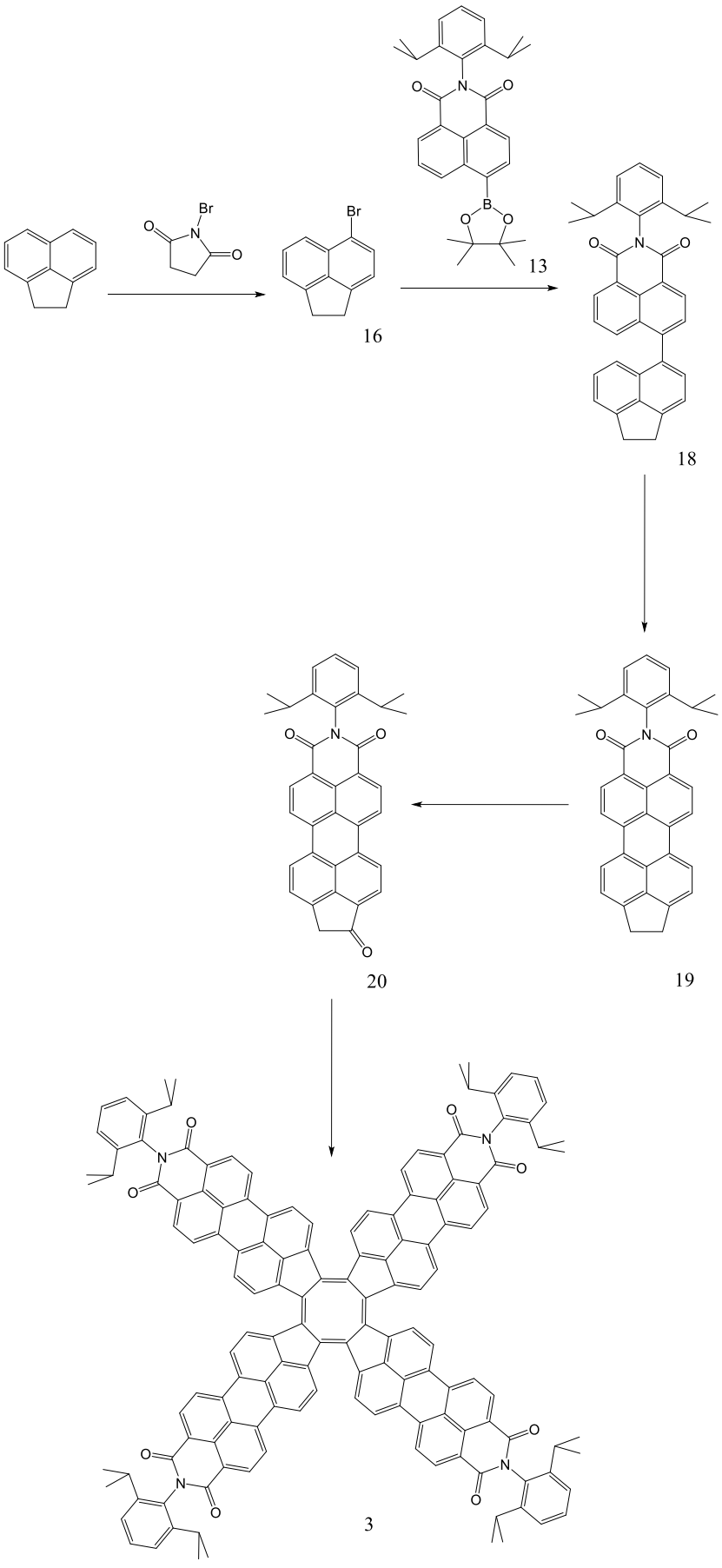

*Figure 3.6 – Alternative synthetic rout for compound **3***

3.2 Characterization

The compounds **1**, **2** and **3'** were characterized by different techniques trying to draw an as complete picture as possible.

At first instance, ^{1}H-NMR was used to prove the succeeding of the reaction steps during the whole period of this project, often in synergy with MALDI-TOF mass spectrometry. For the final products, also a ^{13}C-NMR was performed (Appendix).

3.2.1 NMR spectra

NMR is a very powerful and useful technique to support organic synthesis by monitoring the products obtained in each reaction step. In this work, though, the use of NMR has brought some problems related to the size of some molecules and also due their extended conjugation and low solubility.

In the case of compound **1**, both ^{1}H-NMR and ^{13}C-NMR don't show signal with sufficient intensity, thus resulting in almost flat spectra(fig. 3.7).

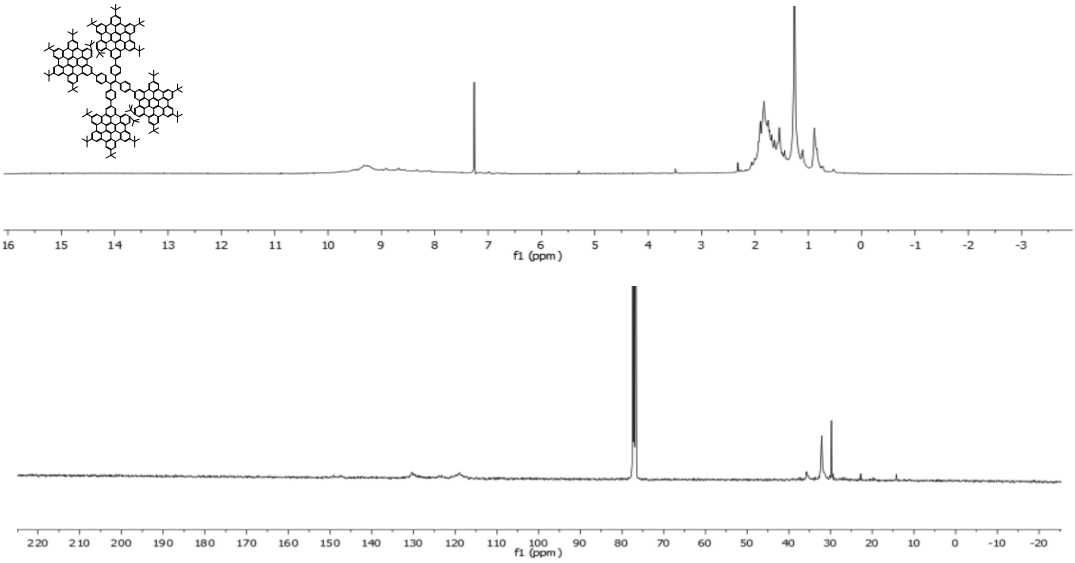

*Figure 3.7 – ^{1}H-NMR and ^{13}C-NMR spectra for compound **1***

It has been envisaged that changing solvent and working with a stronger NMR magnet could help avoid this phenomenon. Accordingly, more experiments will be carried on in a future project.

It is interesting the comparison between compound **15** and **2**. As already explained, from the first compound reaction is possible to obtain the second through a Scholl reaction. In fact, keeping the signal of the solvent as referment it is possible to see that the signals of the majority of the aromatic hydrogens of

the HBC ring in the second spectrum are not visible (the signals in the right side of the spectrum)(fig. 3.8).

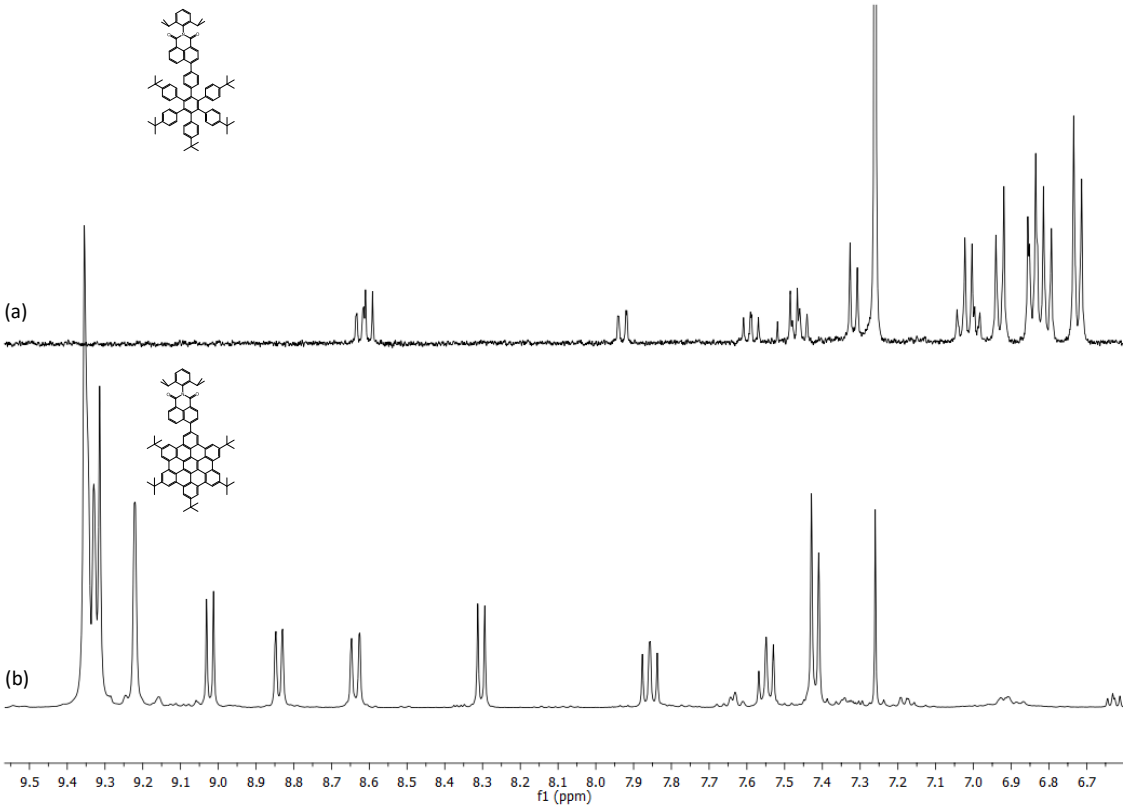

*Figure 3.8 – ^{1}H-NMR spectra of compounds **15** (a) and **2** (b)*

For what concerns the compound **3'**, the spectra is not indicative due to one important fact. It has already been said that the reaction of bromination of acenaphthene derivatives is a simple reaction if it is carried out at temperature condition: the resulting product is mono substituted. The problem is that it is not possible to control in which position the bromine atom goes. This results in a mixture of different isomers. Moreover, in this case, the molecule is composed by four acenaphthene substituents increasing the number of isomers. The ^{1}H NMR spectrum (fig. 3.9c) shows the aromatic signals not defined and instead very complex, making impossible any further elaboration.

However, a work of comparison is still possible. In fig. 3.9, it is possible to see respectively the spectra of compounds **16**, **17** and **3'** showing the development of the synthesis. The region shown is the aromatic one.

The molecule **17** derives from the reaction of bromination of molecule **16**. So, from a symmetrical starting molecule, one not symmetrical is obtained because

of the different possible reaction sites, resulting in a spectrum with already not clear signals.

The final spectrum presents more signals than the ones of the precursor molecules. As already mentioned, molecule **3'** is present in a mixture of different isomers but more than this, it has been functionalised starting from compound **13**, expanding the conjugation and increasing the mass of it, introducing two more factors that influence the quality of the spectrum.

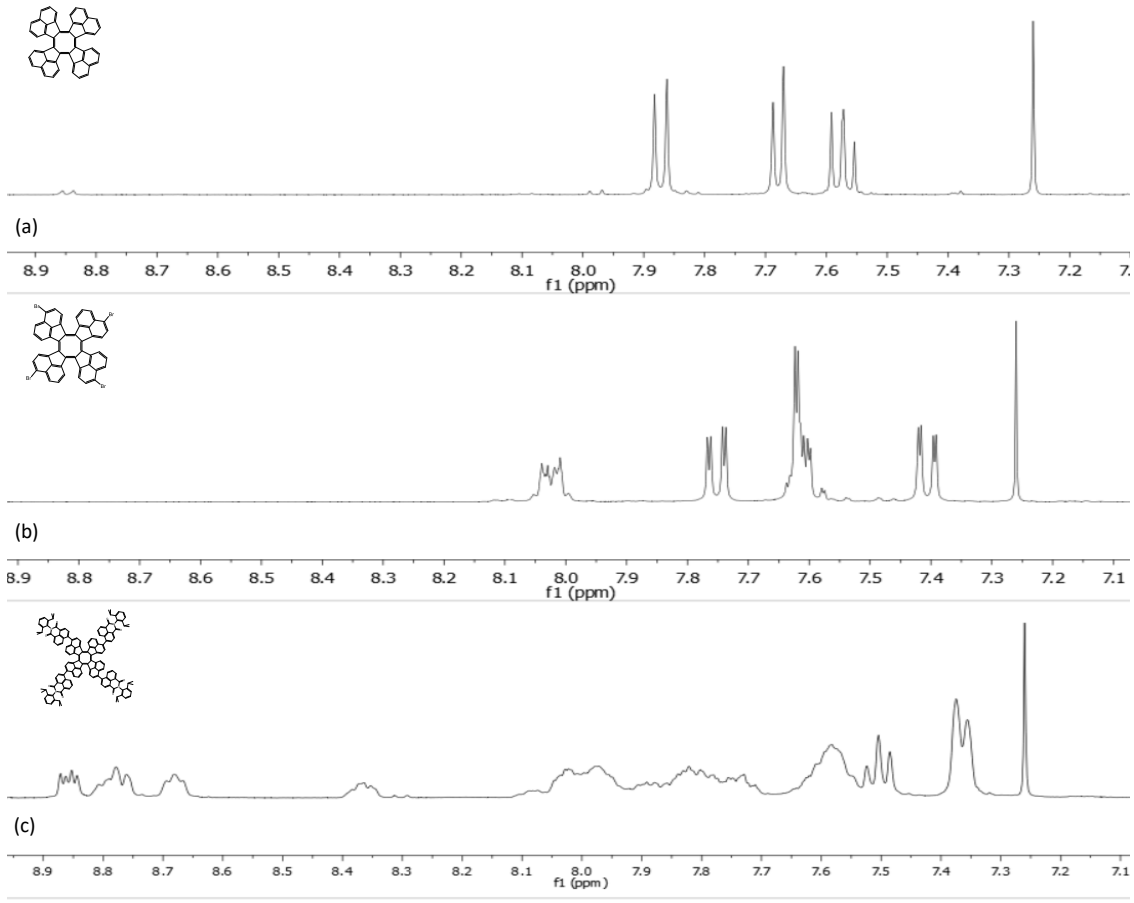

*Figure 3.9 – ^{1}H-NMR spectra of compounds **16** (a), **17** (b) and **3'** (c)*

Speaking of extended conjugation, it has been mentioned that the presence of it can interfere in the experiment giving rise to complex spectra (fig. 3.10). In fact, an extended conjugation gives rise the possibility of stacking of the molecules even causing a possible partial insolubility.

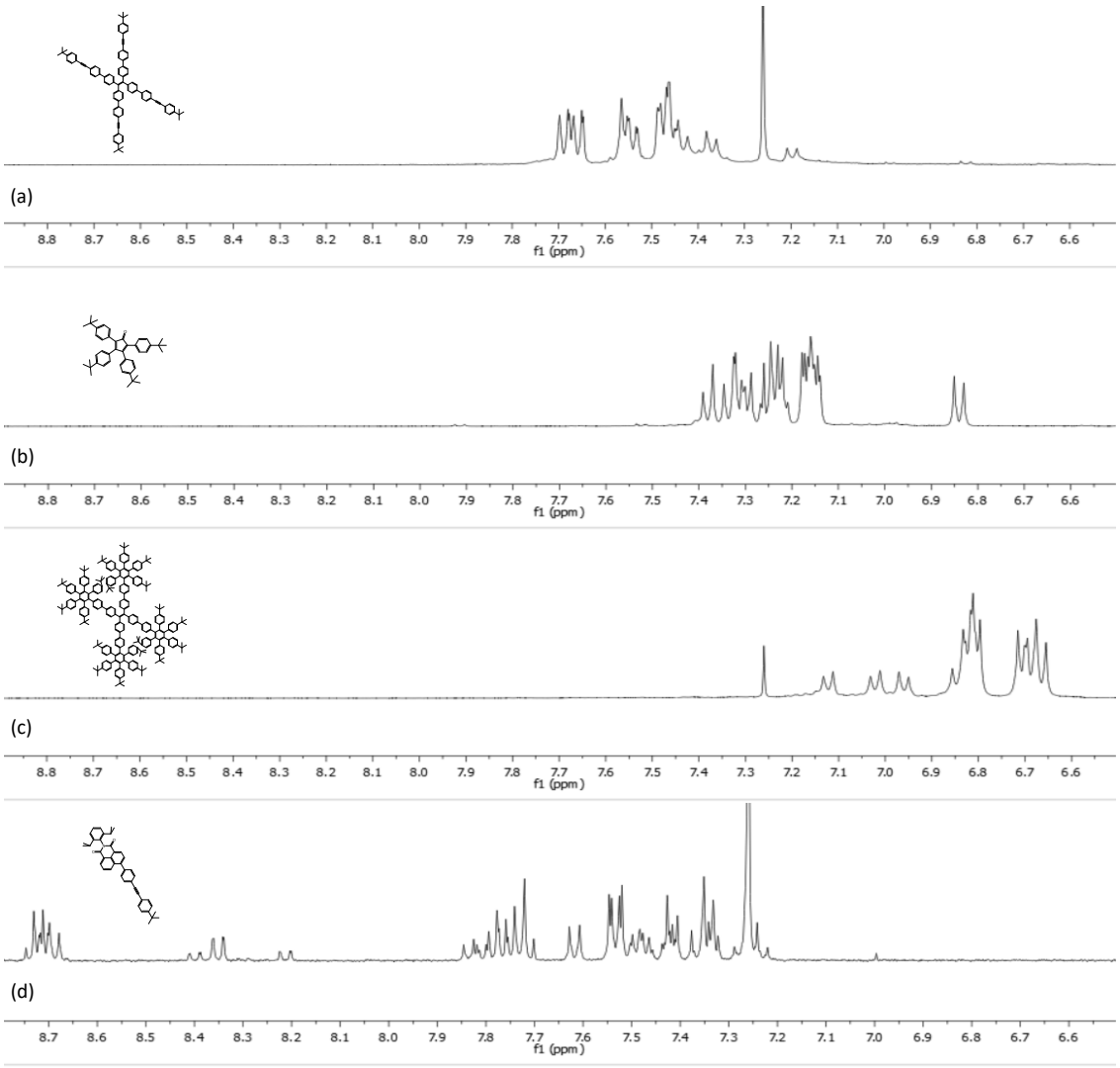

*Figure 3.10 – ^{1}H-NMR spectra of compounds **6** (a), **10** (b), **11** (c) and **14** (d)*

3.2.2 Absorbance and fluorescence

The optical characteristics of compounds **1**, **2**, and **3'** were investigated by means of steady-state absorption spectroscopy and emission spectroscopy using DCM as solvent.

The absorbance and emission data were present together in same spectra after being normalised (fig. 3.11)

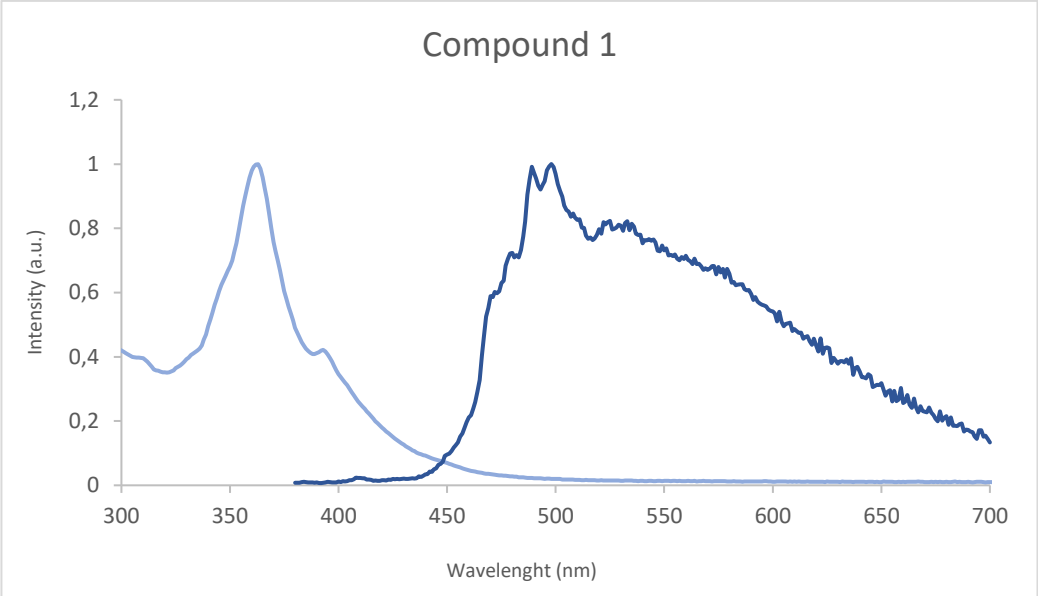

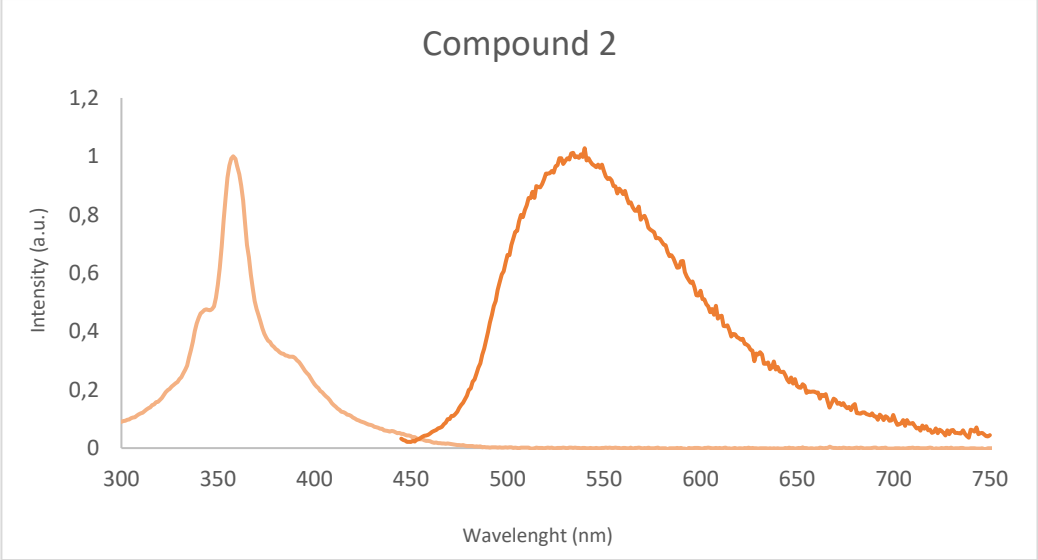

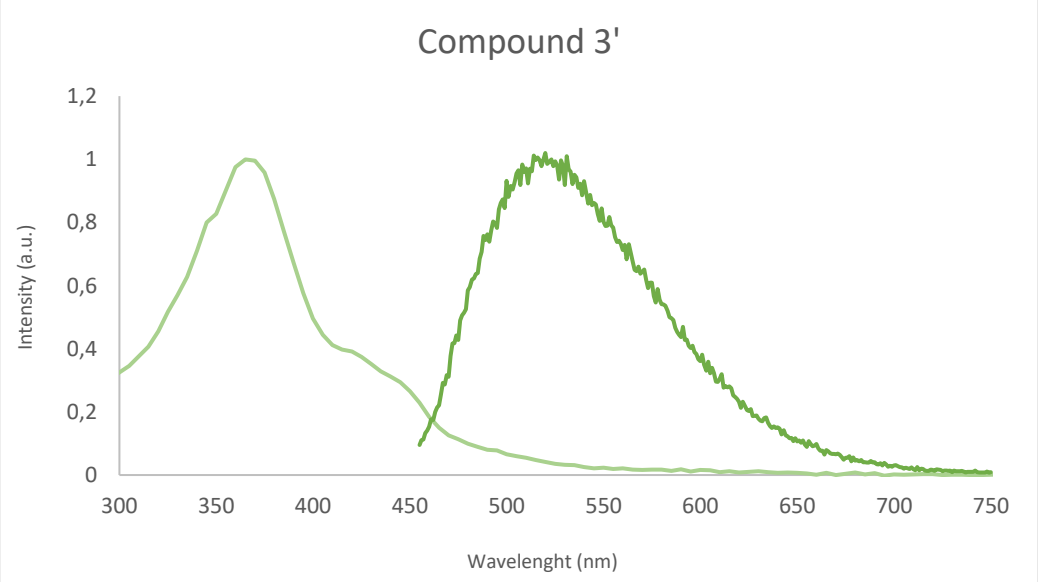

*Figure 3.11 – Absorption and emission spectra normalised of compounds **1, 2, 3'***

The absorption spectrum of **1** features an absorption maximum peaked at 362 nm with additional fine structure at 346 and 394 nm. These two signal are characteristic of the HBC ring. The emission spectrum show two thin peaks at 490 and 497 nm.

The absorption spectrum of **2** possesses characteristic absorption maximum at 359 nm, and similar features of compound 1 at wavelengths of 346 and 390 nm. Here, the emission spectrum is a broad band with a maximum at 536 nm.

The absorption spectrum of compound **3'** shows a thin band peaked at 370 nm. The emission spectrum is a broad band with a maximum at 523 nm.

The high level of conjugation of these three molecules make them a perfect example of chromophore molecules and even fluorophore molecules.

From the spectrum, it is possible to calculate the energy gap between HOMO and LUMO, using a simple equation

$$E_{gap} = \frac{1240}{wavelenght} \qquad [eV]$$

So, since the intersection between the absorption and emission occurs at 448 nm, it is possible to affirm that the band gap energy values 2.78 eV.

3.2.3 Aggregation-Induced Emission (AIE)

From **1**, it was possible to observe a slight luminescence in solid state. Because of it, it was decided to perform experiments of emission to test the aggregation-induced emission (AIE). The central scaffold of compound **1** is the tetraphenylethene, which is well-known for exhibiting aggregation-induced emission. This effect is attributed to the result of the restriction of the rotation and vibration of a part of the molecules that in solution result in non-radiative relaxation processes.

The experiment consists in making ten solutions with the same concentration (~10^{-6} M, data obtained from experiment of absorption) varying the ratio between two solvents, in this case THF and water.

If normally increasing the fraction of the bad solvent results in a quench of the emission, due to the aggregation, here the aggregation induces an increase of

emission intensity, i.e. compound **1** exhibites a green fluorescence arising from the HBC counterparts.

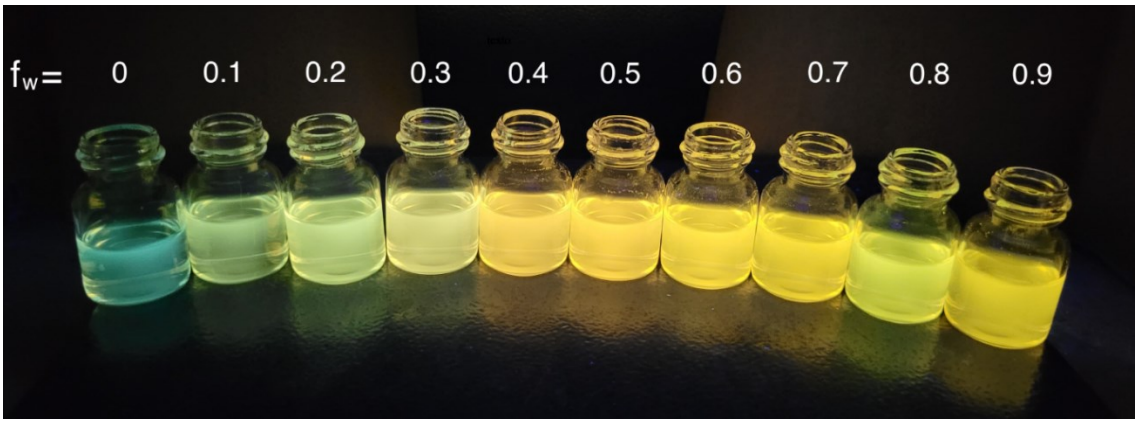

Figure 3.12 – Picture of the solutions with the variation in luminescence depending on f_w

When the molar fraction of THF is decreasing (0.9) the fluorescence of compound **1** is slightly quenched. This trend continues until reaching a THF molar fraction of 0.8, where the previous band at 490 nm becomes a shoulder of a new red-shifted broad emission band appeared at 570nm. At even higher dilution (between 0.7 and 0.1 of THF) the shoulder disappear and it is observed a broad band with higher intensity at the same wavelength (fig 3.13).

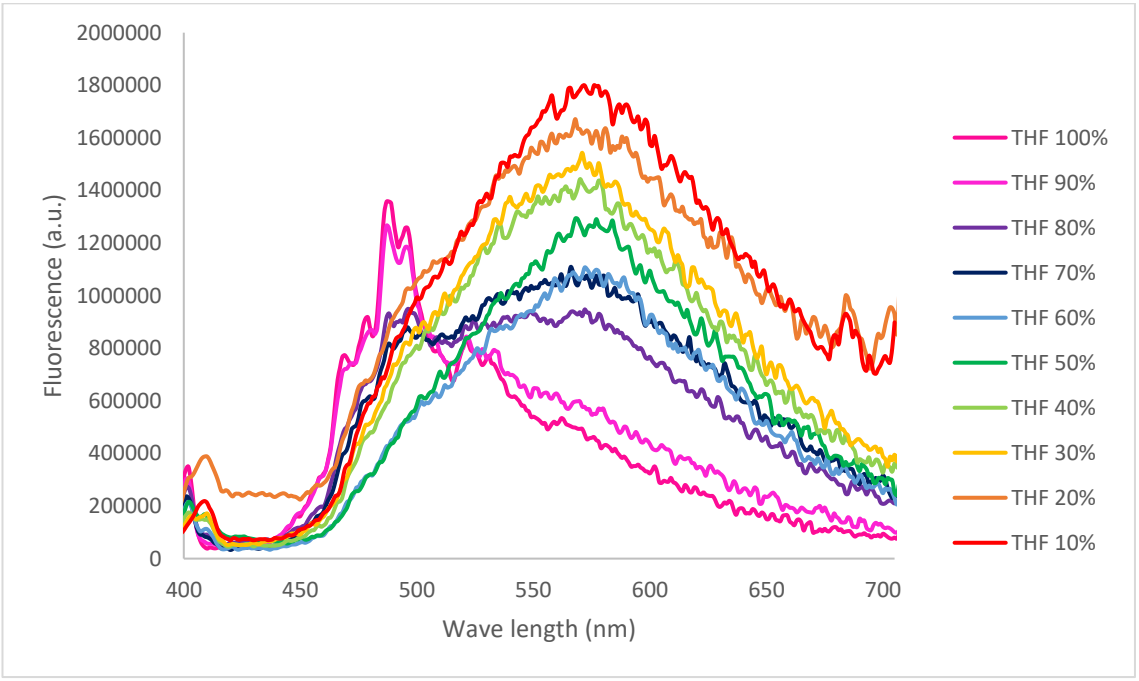

Figure 3.13 – Emission spectrum of AIE phenomenon

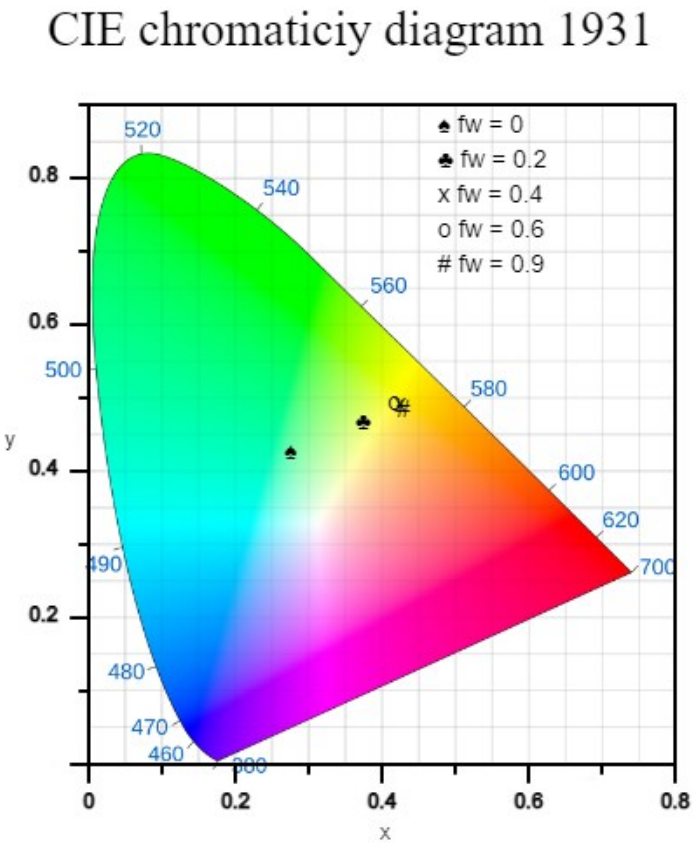

Figure 3.14 – The chromaticity chart shows how the colour of the emission varies depending on the fraction on water (f_w), from a cyan colour the emission moves to a yellow one

Taking into account the molecular structure of compound **1**, the HBC groups have rotational and vibrational freedom in solution. When a bad solvent, such as water, is added, the HBC groups of different molecules start to undergo π-π interactions with the consequent formation of aggregates and the increase of the fluorescence quantum yield.

3.2.4 Cyclic voltammetry

The electrochemical properties of ^{t}Bu-HBC (fig. 3.15) and compound **1** were explored by cyclic voltammetry. In the following voltammogram (fig. 3.16), it is possible to see the performance of both of them.

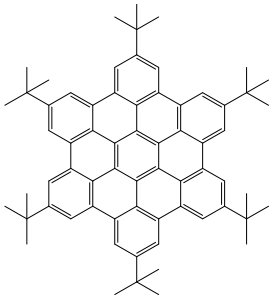

Figure 3.15 – ^{t}Bu-HBC

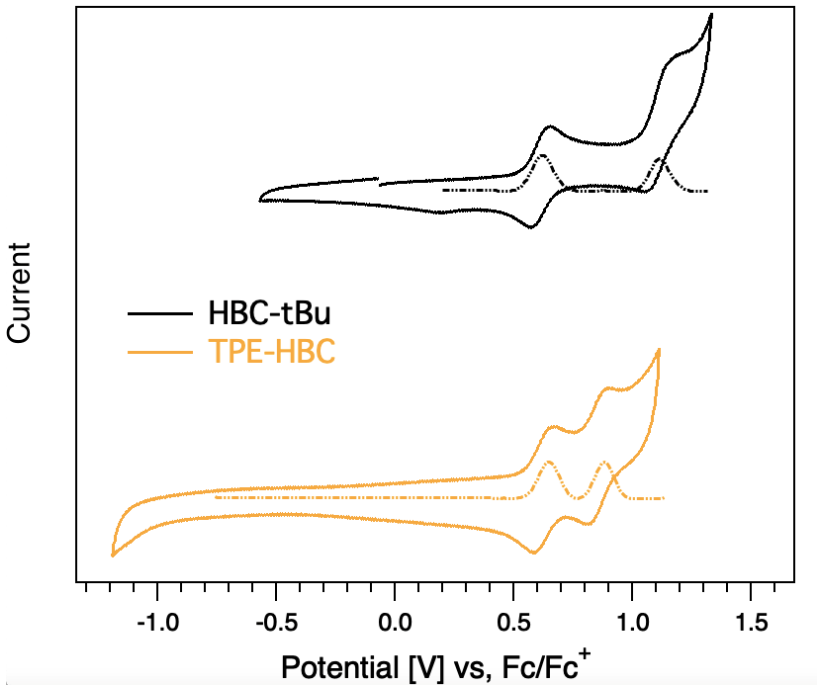

Figure 3.16 – Cyclic voltammogram of ᵗBu-HBC and TPE-HBC

The experiments were performed in tetrabutylammonium hexafluorophosphate 0.1 M solution as the supporting electrolyte and the results obtained were referred to Fc/Fc^{+}.

The cyclic voltammogram of ᵗBu-HBC was performed in a range of potential between -0.6 and +1.3 V. It shows two forward and reverse wave and the two oxidation peaks lie at +0.65 and +1.1 V. The half wave potential of the first wave measured as

$$E_{1/2} = \frac{E_{ox} + E_{red}}{2} \quad [V]$$

values +0.58 V.

The cyclic voltammogram of compound **1** was performed in a range of potential between -1.2 and +1.1 V. It shows two forward and reverse wave and the two oxidation peaks lie at +0.68 and +0.89 V. The half wave potential of the first wave values 0.64 V.

Hence, it is possible to affirm that the peaks of oxidation in the upper part are positioned at potential close to the one of the reduction peaks, with just a small difference. This is a sign of the reversibility of the process. Actually, the reversibility of the process is an important characteristic for suitable compound

for electronic devices, because they have to overcome to a number of redox processes during the device life cycle.

With this experiment, it is not possible to know how many electrons the molecules can donate during the oxidation process (the same for the electron accepted during the reduction process), but it is possible to calculate the energy of the HOMO from the first oxidation potential following a simple equation:[38]

$$E_{HOMO} = \left(E_{ox} - E_{1/2(ferrocene)}\right) + 4.8\ [eV]$$

Where E_{Ox} is the energy of the oxidation obtained from the voltammogram and $E_{1/2(ferrocene)}$ is the half wave potential of the ferrocene.

Keeping the approximated value of 0.2 V for $E_{1/2(ferrocene)}$ and the already seen value of E_{Ox} from the voltammogram, the resulting HOMO energy is equal to 5.28 eV.

Knowing the energy gap calculated from the intersection between absorption and emission spectrum, it is possible to obtain the LUMO energy:

$$E_{LUMO} = E_{HOMO} + E_{gap}$$

obtaining a LUMO energy equal to 8.06 eV.

*Table 1 – Table containing resuming data of compound **1***

	E_{ox}	E'_{ox}	E_{red}	E'_{red}	E_{HOMO}	E_{LUMO}	$E_{band\ gap}$
TPE-HBC	+0.68 V	+0.89 V	+0.60 V	+0.85 V	5.28 eV	8.06 eV	2.78 eV

4 Conclusions

We are living in a very delicate period. If it is true that science and technology are showing their best, it is also true that the Earth is struggling because of the global warming.

This brought the scientific community to study technologies in order to fight this problem and to give society a greener future. Thanks to this, renewable energies were born and different fields started to study them.

In this thesis work, the green energy taken in account is solar energy. In fact, the purpose of this project is to study the synthesis of three organic molecules sharing specific features, useful for the improvement of performances of perovskite solar cells.

The most relevant feature, found in all these compounds, is a broad conjugation that brings with it different fundamental properties, such as electronic and optical behaviour.

Conjugation allows electrons to move freely through the molecule, that can assume a donor or acceptor character depending on the functionalization. This gives the possibility to tune the behaviour of such a highly conjugated compound, making it a suitable material for HTL or ETL respectively.

The chemistry at the basis of the synthesis is willingly common chemistry in view of a possible future industrialization. Therefore, the reactions used are palladium catalysed reaction such as Suzuki – Miyaura coupling reaction, Diels – Alder reaction and Scholl reaction. All of these are commonly used in organic synthesis to create new C-C bonds and to increase the degree of conjugation of the target molecule.

After the synthesis, a thorough characterization work has been carried on. Firstly, common techniques such as ^{1}H and ^{13}C-NMR and mass spectrometry have been used to monitor the success of each synthetic step. Then, the three final compounds have been characterised deeply through experiments of UV-Vis spectroscopy and cyclic voltammetry.

About UV-Vis spectroscopy, experiment of absorption and emission have been performed. More in detail, compound **1** and **2** show similar absorption spectra with features common in the HBC ring. In fact, the spectra feature an absorption maximum peaked at 360 nm with additional fine structures at 346 and 390 nm.

Compound **3'** shows a broader peak at 370 nm. Regarding the emission spectra, it has been said that all the three target compounds show a good emission because of the extended conjugation, which makes them optimal chromophore and even fluorophore compounds.

For compound **1**, an interesting phenomenon called AIE has been observed. Thanks to this, the compound shows luminescence in the solid state and more in general in the aggregated state, making it a useful molecule for more applications, such as OLEDs.

Through cyclic voltammetry it has been possible to evaluate the electrochemical characteristics of compound **1** also in comparison with ^{t}Bu-HBC. From the oxidation potential it has been possible to calculate an approximated value of HOMO energy and, summing it with the energy of band gap obtained from the interception of absorption and emission spectra, it has been possible to calculate the LUMO energy, too.

In conclusion, in this work three interesting compounds have been studied with a possible key role in the developing of future devices such as organic and hybrid photovoltaics cell and OLEDs. Therefore, further investigations on these and derived compounds have been planned for a following PhD project.

5 Bibliography

1 R. A. Pielke Jr, *Energy & environment*, **2004**, 15, 3

2 M. Höök, X. Tang, *Energy Policy*, **2013**, 23, 797-809

3 H. Ritchie, P Rosado, Our World in Data, 2017

4 I. Dinçer, C. Zamfirescu, Sustainable energy system and applications, Spinner Science + Business Media, **2011**

5 C. Langmuir, *EOS*, **1999**, 80, 39

6 A. M. Omer, *Renewable and sustainable energy reviews*, **2008**, 12, 1789-1821

7 B. Kippelen, J. Brédas, *Energy Environ. Sci.*, **2009**, 2, 251-261

8 C. W. Tang, *Appl. Phys. Lett.*, **1986**, 48, 183

9 Y. Rong, Y. Hu, A. Mei, H. Tan, M. I. Saidaminov, S. I. Seok, M. D. McGehee, E. H. Sargent, H. Han, *Science*, **2018**, 361, 1-7

10 G. Yang, H. Tao, P. Qin, W. Ke, G. Fang, *J. Mater. Chem. A*, **2016**

11 K. Mahmood, S. Sarwar. M. T. Mehran, *RSC. Adv.*, **2017**, 7, 17044-17062

12 C. Anrango-Camacho, K. Pavón-Ipiales, B. A. Frontana-Uribe, A. Palma-Cando, *Nanomaterials*, **2022**, 12

13 G. Tumen-Ulzii, T. Matsushima, C. Adachi, *Energy Fuels*, **2021**, 35, 18915-18927

14 B. A. Gregg, *J. Phys. Chem. B*, **2003**, 107, 4688-4698

15 J. Nelson, *Current Opinion in Solid State and Materials Science*, **2002**, 6, 87-95

16 J. C. Bernède, *J. Chil. Chem. Soc.*, **2008**, 53, 1549-1564

17 M. Bacon, S. J. Bradley, T. Nann, *Part. Part. Syst. Charact.*, **2014**, 31, 415-428

18 J. M. Fernández-García, P. J. Evans, S. Filippone, M. Á. Herranz, N. Martín, *Acc. Chem. Res.*, **2019**, 52, 1565-1574

19 A. Narita, X. Wang, X. Feng, K. Müllen, *Chem. Soc. Rev.*, **2015**, 44, 6616-6643

20 J. McMurry, Organic Chemistry, Eighth Edition, **2012**, Brooks/Cole, Cengage Learning

21 R. A. Abramovitch, *The new Journal for organic synthesis*, **1991**, 23, 6, 685-711

22 A. J. J. Lennox, G. C. Lloyd-Jones, *Chem. Soc. Rev.*, **2014**, 43, 412-443

23 N. Miyaura, A. Suzuki, *Chem. Rev.*, **1995**, 95, 2457-2483

24 R. S. Jassas, E. U. Mughal, A. Sadiq, R. I. Alsantali, M. M. Al-Rooqi, N. Naeem, Z. Moussa, S. A. Ahmed, *RSC Adv.*, **2021**, 11, 32158-32202

25 R. Scholl and J. Mansfeld, *Ber. Dtsch. Chem. Ges. A*, **1910**, 43, 1734-1746

26 B. T. King, J. Kroulík, C. R. Robertson, P. Rempala, C. L. Hilton, J. D. Korinek, L. M. Gortari, *J. Org. Chem.*, **2007**, 72, 2279-2288

27 D. J. Jones, B. Purushothaman, S. Ji, A. B. Holmes, W. W. H. Wong, *Chem. Comm.*, **2012**, 48, 8066-8068

28 Y. Hong, J. W. Y. Lam, B. Z. Tang, *Chem. Soc. Rev.*, **2011**, 40, 5361-5388

29 A. B. S. Elliot, R. Horvath, X. Sun, M. G. Gardiner, K. Müllen, N. T. Lucas, M. W. George, K. C. Gordon, *Inorg. Chem.*, **2016**, 55, 10, 4710-4719

30 E. K. Perttu, M. Arnold, P. M. Iovine, *Tetrahedron Lett.*, **2005**,46, 50, 8753-8756

31 H. Wei, X. Ma, L. Gu, J. Li, W. Si, G. Ou, W. Yu, C. Zhao, J. Li, M. Song, Z. Peng, H. Wu, *J. Org. Chem.*, **2016**, 81, 3839-3847

32 A. D. D. Wonake, J. L. Ferguson, C. M. Fitchett, D. L. Crittenden, *Chemistry, Asian Journal*, **2019**, 14, 1293-1303

33 N. Meitinger, A. K. Mengele, K. Witas, S. Kupfer, S. Rau, D. Nauroozi, *Eu. J. Org. Chem.*, **2020**, 42, 6555-6562

34 R. Nagpal, S. Arora, P. Ponnan, K. Nisa, A. Dandia, S. M. S. Chauhan, *ChemistrySelect*, **2019**, 4, 8444-8449

35 A. R. Mallia, M. Hariharan, *J. Phys. Chem. C*, **2017**, 121, 4778-4788

36 G. Zhang, H. Wang, M. P. Aldred, T. Chen, Z. Chen, X. Meng, M. Zhu, *Chem. Mater*, **2014**, 26, 4433-4446

37 H. Seyler, B. Purushothaman, D. J. Jones, A. B. Holmes, W. W. H. Wong, *Pure Appl. Chem.*, **2012**, 84, 4, 1047-1067

38 A. Shafiee, M. M. Salleh, M. Yahaya, *Sains Malaysiana*, **2011**, 40, 2, 173-176

Appendix

^{1}H and ^{13}C-NMR

Compound **1**

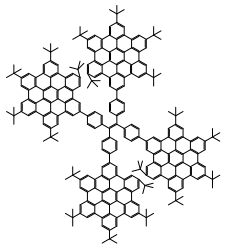

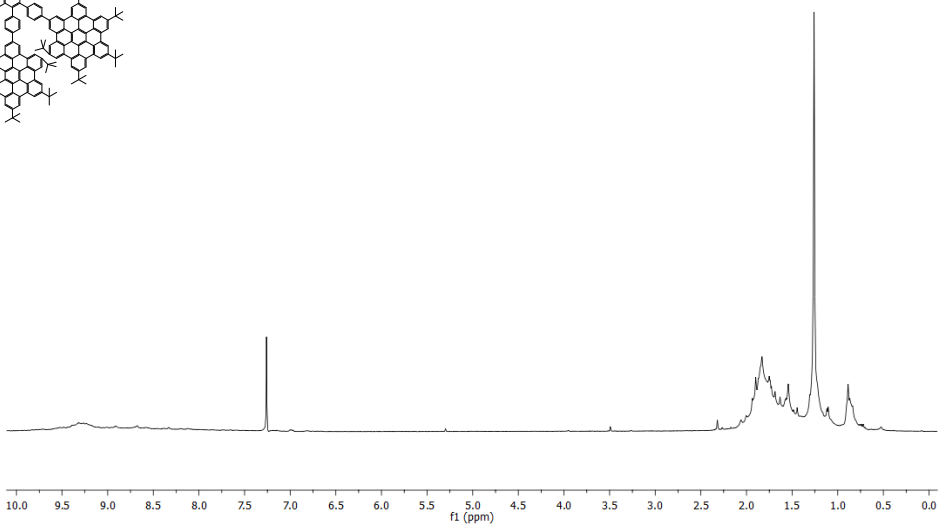

^{1}H NMR (400 MHz, $CDCl_3$): n/a

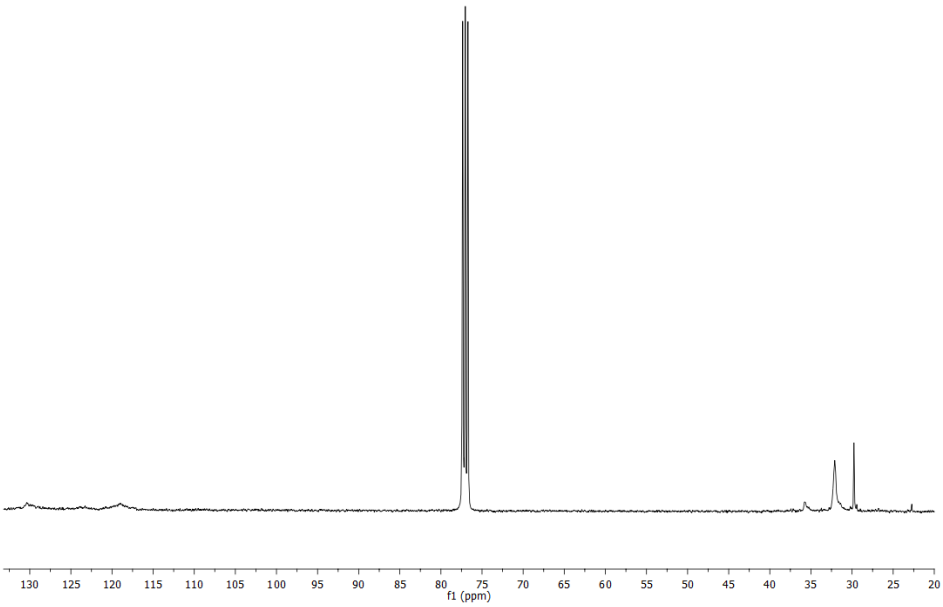

^{13}C NMR (101 MHz, $CDCl_3$): δ (ppm) 77.38, 77.35, 77.06, 77.03, 76.71, 32.10, 29.77

Compound **2**

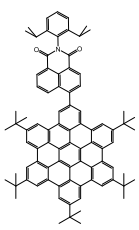

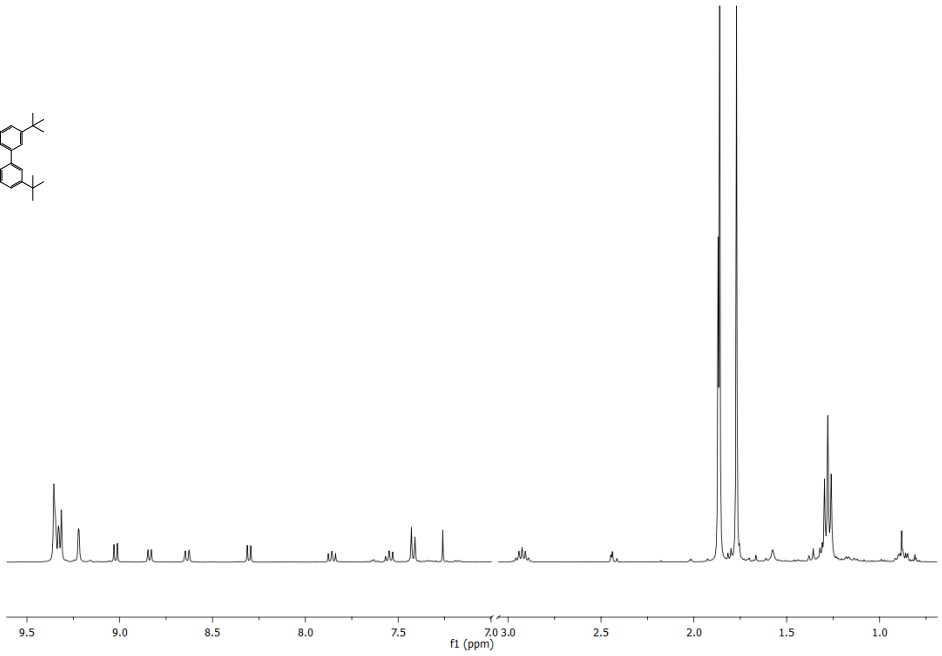

^{1}H NMR (400 MHz, $CDCl_3$): δ (ppm) 9.37-9.30 (m, 1H), 9.22 (s, 1H), 9.02 (d, J = 7.4 Hz, 1H), 8.84 (d, J = 7.2 Hz, 1H), 8.64 (d, J = 8.6 Hz, 1H), 8.30 (d, J = 7.4 Hz, 1H), 7.86 (dd, J = 8.4, 7.3 Hz, 1H), 7.58-7.52 (m, 1H), 7.42 (d, J = 7.7 Hz, 1H), 2.98-2.86 (m, 1H), 1.85-1.0 (s, 57H).

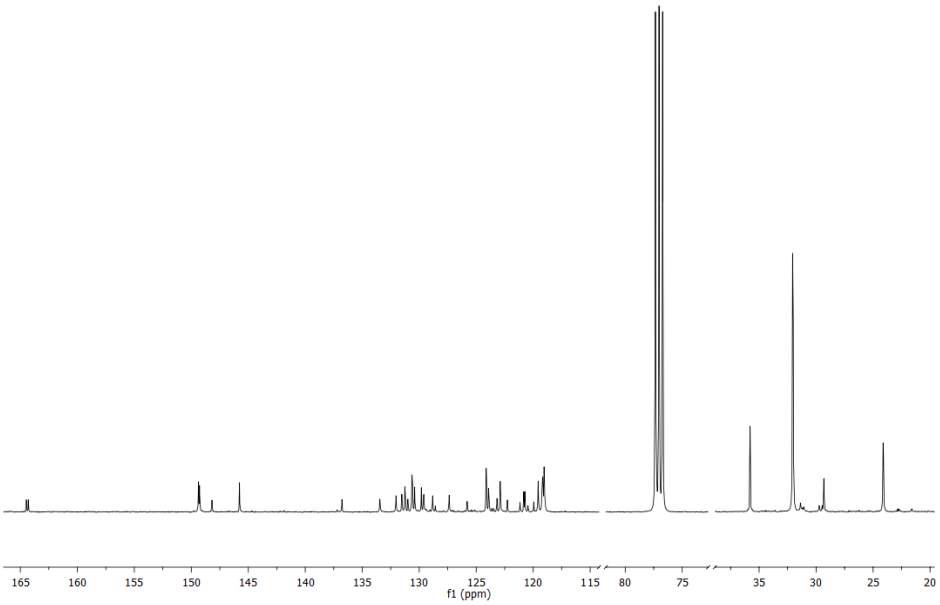

^{13}C NMR (101 MHz, $CDCl_3$): δ (ppm) 164.45, 164.27, 149.36, 149.28, 148.17, 145.77, 136.72, 133.38, 131.97, 131.49, 131.22, 130.96, 130.61, 130.35, 129.77,

129.54, 128.76, 124.06, 121.12, 119.93, 119.18, 119.04, 77.35, 77.04, 76.72, 35.79, 32.03, 29.27, 24.11

Compound **3'**

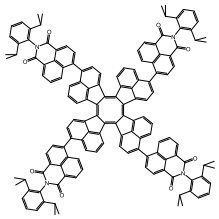

^{1}H NMR (400 MHz, $CDCl_3$): δ (ppm) 8.9-7.3 (m, 52H), 1.30-1.10 (m, 48H)

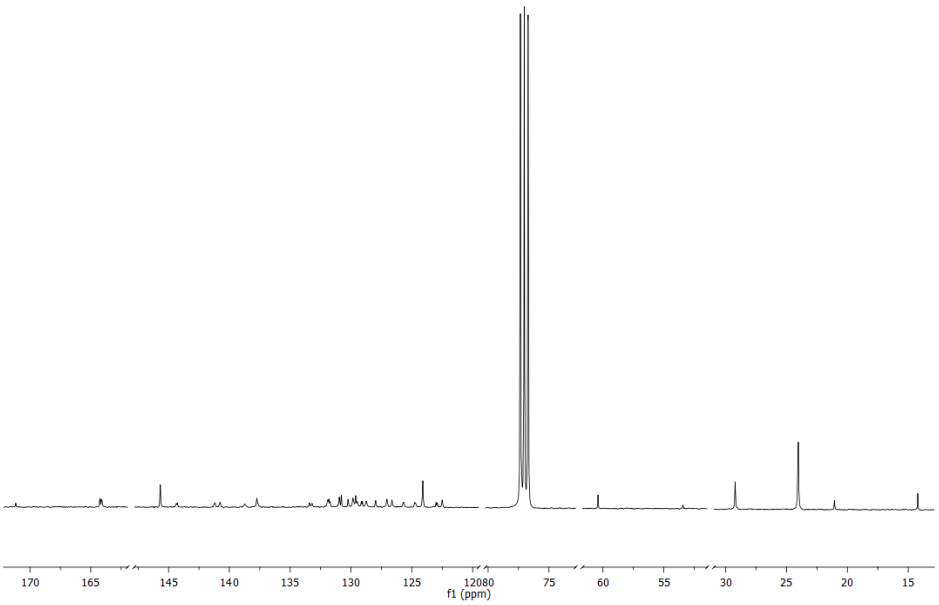

^{13}C NMR (101 MHz, $CDCl_3$): δ (ppm) 171.16, 164.23, 164.12, 164.07, 145.67, 144.33, 141.19, 140.76, 137.74, 133.41, 133.18, 131.89, 131.81, 131.73, 130.97,

130.80, 130.25, 129.14, 128.75, 125.68, 77.35, 77.03, 76.71, 60.41, 29.23, 24.03, 21.06, 14.21

Compound **4**

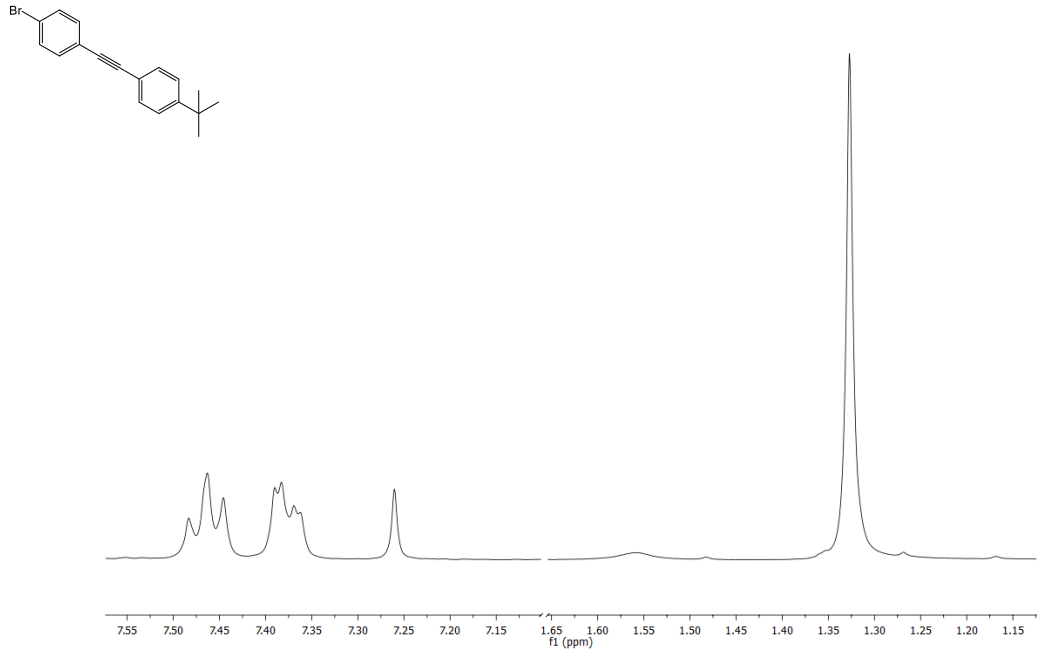

^{1}H NMR (500 MHz, $CDCl_3$): δ (ppm) 7.47 (d, J = 8.5 Hz, 2H), 7.45 (d, J = 8.2 Hz, 2H), 7.38 (d, J = 8.8 Hz, 2H), 7.37 (d, J = 8.8 Hz, 2H), 1.33 (s, 9H)

Compound **5**

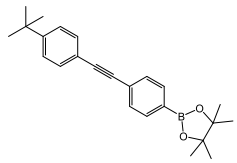

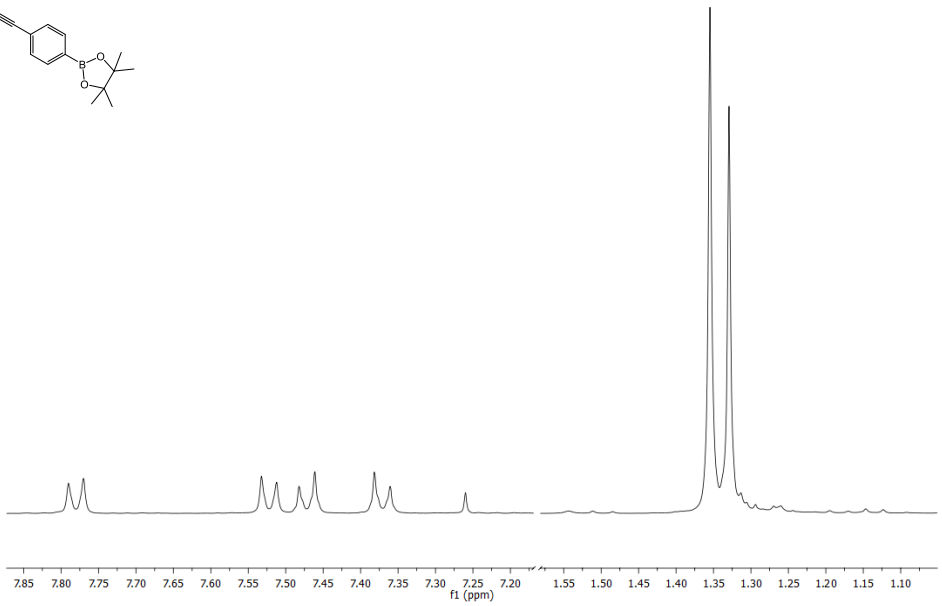

^{1}H NMR (500 MHz, $CDCl_3$): δ (ppm) 7.78 (d, J = 8.1 Hz, 2H), 7.52 (d, J = 8.1 Hz, 2H), 7.47 (d, J = 8.4 Hz, 2H), 7.37 (d, J = 8.4 Hz, 2H), 1.36 (s, 12H), 1.33 (s, 9H)

Compound **6**

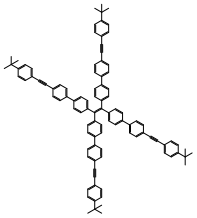

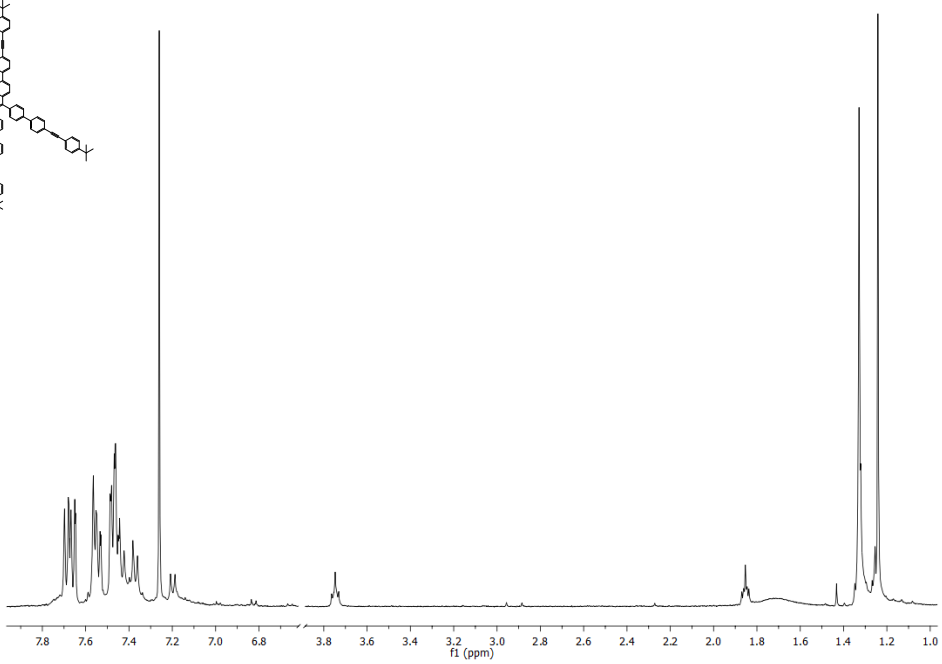

^{1}H NMR (400 MHz, $CDCl_3$): δ (ppm) 7.70-7.15 (m, 48H), 1.25 (s, 36H)

Compound **7**

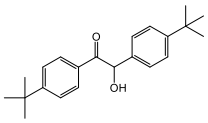

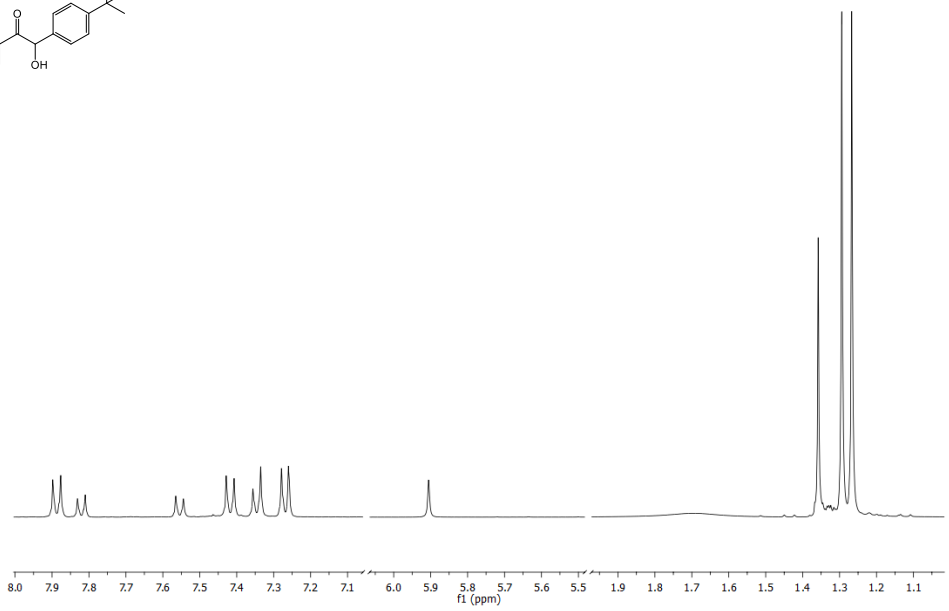

^{1}H NMR (300 MHz, $CDCl_3$): δ (ppm) 7.87 (d, J = 8 Hz, 2H), 7.40 (d, J = 8 Hz, 2H), 7.34 (d, J = 8 Hz, 2H), 7.27 (d, J = 8 Hz, 2H), 5.90 (s, 1H), 1.36 (s, 9H), 1.40 (s, 9H)

Compound **8** LCA007

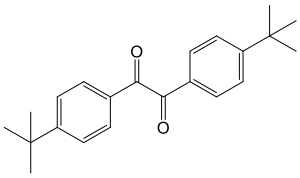

^{1}H NMR (400 MHz, $CDCl_3$): δ (ppm) 7.91 (d, J = 8.8 Hz, 4H), 7.52 (d, J = 8.8 Hz, 4H), 1.29 (s, 18H)

Compound **9**

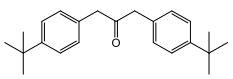

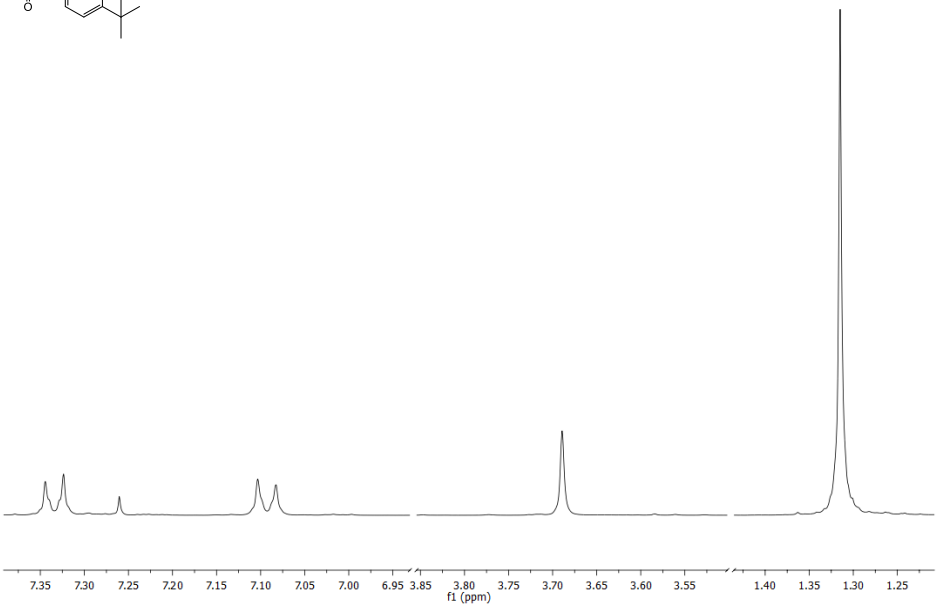

^{1}H NMR (400 MHz, $CDCl_3$): δ (ppm) 7.37 (d, J = 8.3 Hz, 4H), 7.13 (d, J = 8.3 Hz, 4H) 3.73 (s, 4H), 1.35 (s, 18H)

Compound **10**

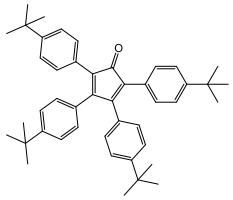

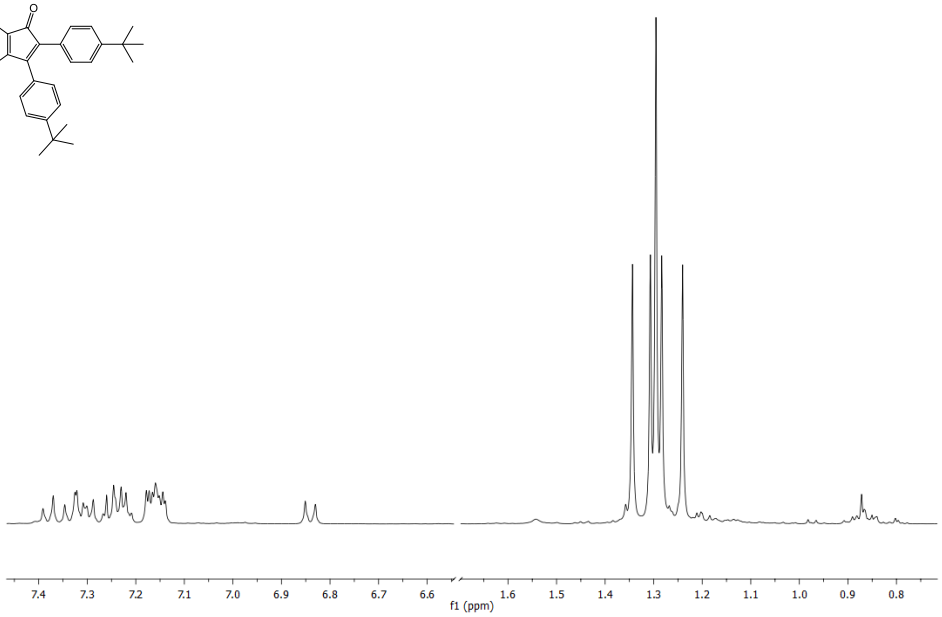

^{1}H NMR (400 MHz, $CDCl_3$): δ (ppm) 7.30 (d, 4H, J=8.0 Hz), 7.25 (d, 4H, J = 8.0 Hz), 7.20 (d, 4H, J=8.0 Hz), 6.70 (d, 4H, J=8.0 Hz), 1.26 (s, 18H,), 1.25 (s, 18H)

Compound **11**

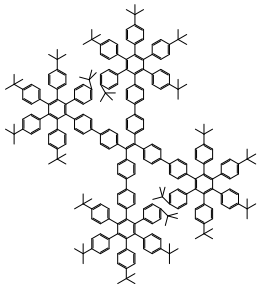

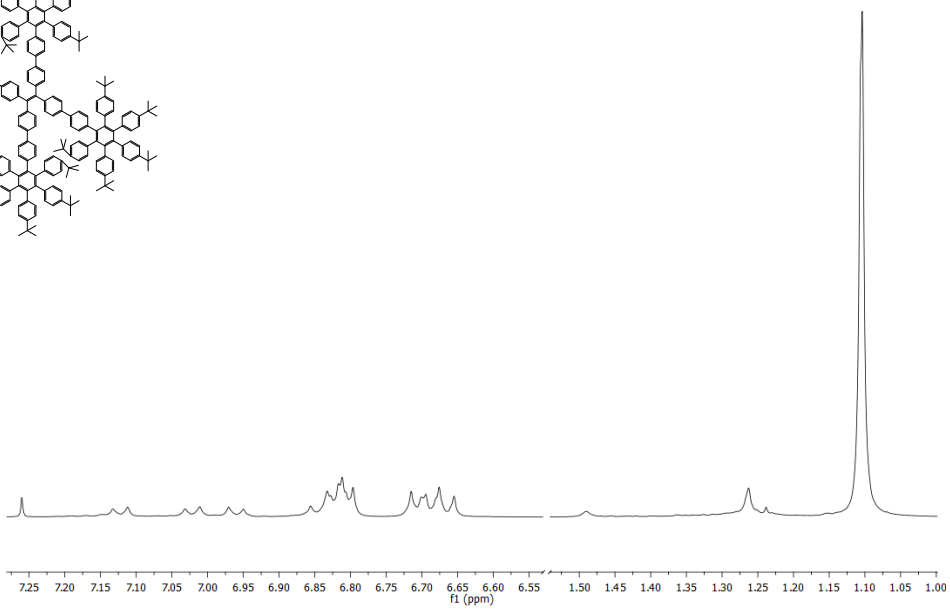

^{1}H NMR (400 MHz, $CDCl_3$): δ (ppm) 7.13 (m, 9H), 6.99 (m, 16H), 6.82 (m, 47H), 6.69 (m, 40H), 1.10 (s, 180H)

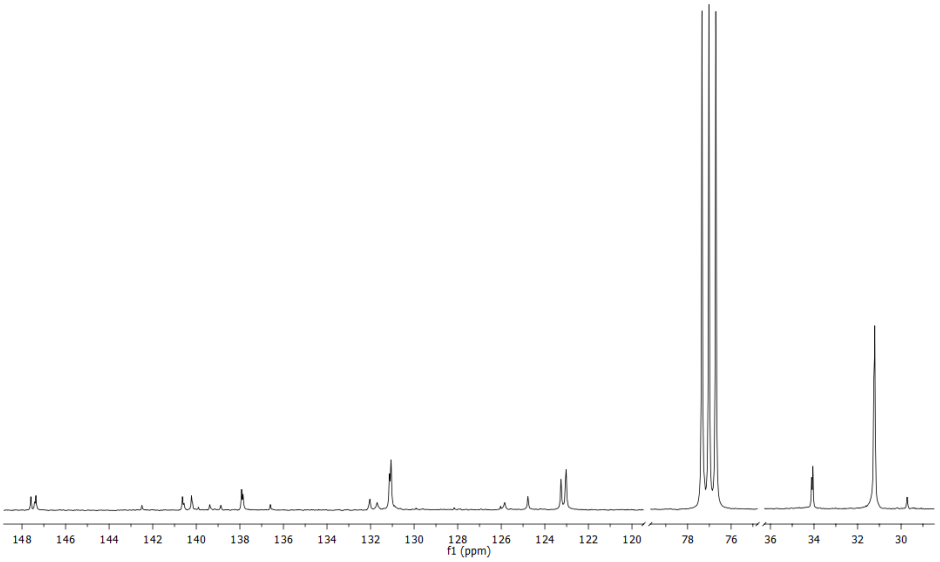

^{13}C NMR (101 MHz, $CDCl_3$): δ (ppm) 147.60, 147.39, 142.50, 140.54, 140.22, 139.39, 138.81, 137.89, 136.53, 132.03, 131.70, 131.10, 125.84, 124.78, 123.26, 123.02, 77.34, 77.02, 76.70, 34.11, 34.05, 31.23

Compound **12**

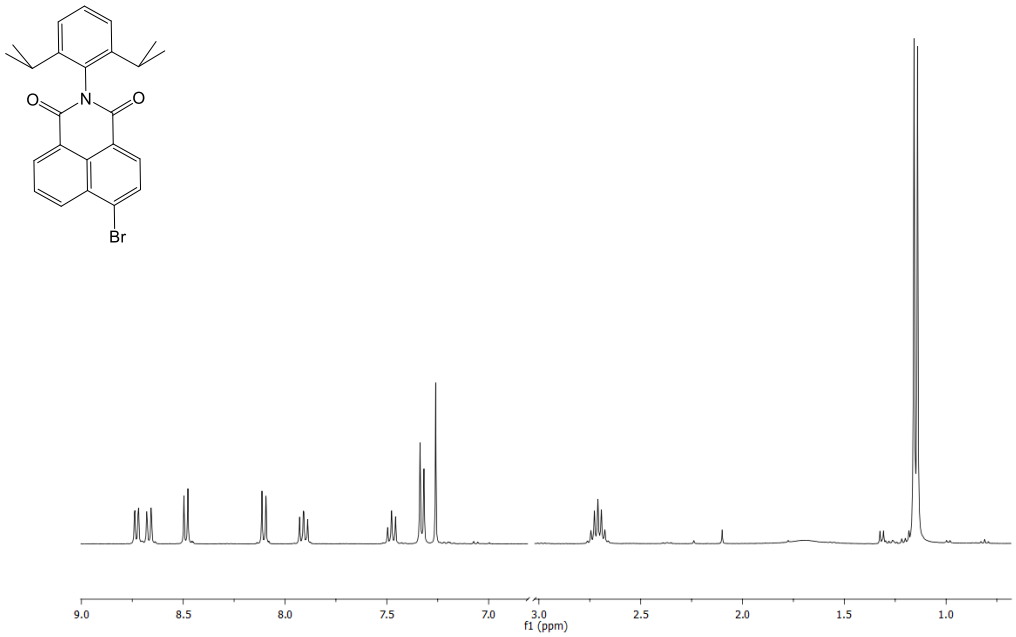

^{1}H NMR (500 MHz, $CDCl_3$): δ (ppm) 8.66 (d, J = 10 Hz, 1H), 8.60 (d, J = 10 Hz, 1H), 8.42 (d, J = 10 Hz, 1H), 8.04 (d, J = 10 Hz, 1H), 7.84 (t, J = 15 Hz, 1H), 7.42 (t, J = 15 Hz, 1H), 7.26 (d, J = 10 Hz, 2H), 2.66 (m, 2H), 1.08 (d, J = 5 Hz, 12H)

Compound **13**

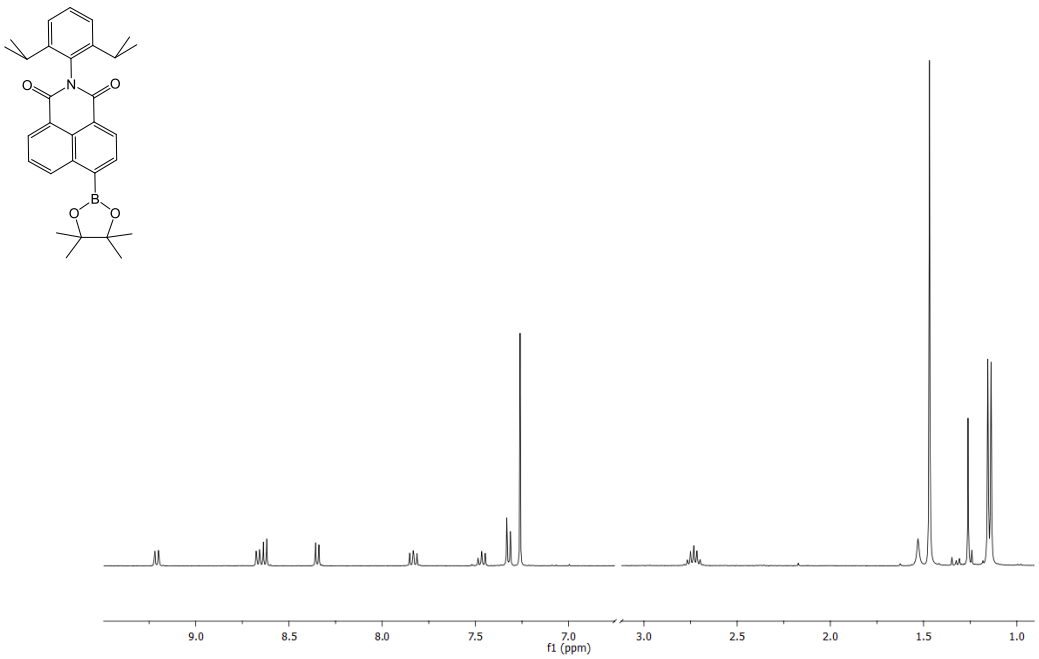

^{1}H NMR (400 MHz, $CDCl_3$): δ (ppm) 9.20 (d, J = 8.4 Hz, 1H), 8.65 (d, J = 7.2 Hz, 1H), 8.62 (d, J = 7.2 Hz, 1H), 8.34 (d, J = 7.2 Hz, 1H), 7.81 (t, J = 7.6 Hz, 1H),

7.45 (t, J = 8.0 Hz, 1H), 7.31 (d, J = 8.0 Hz, 2H), 2.70 (m, 2H), 1.47 (s, 12H), 1.14 (d, J = 6.8 Hz, 12H)

Compound **14**

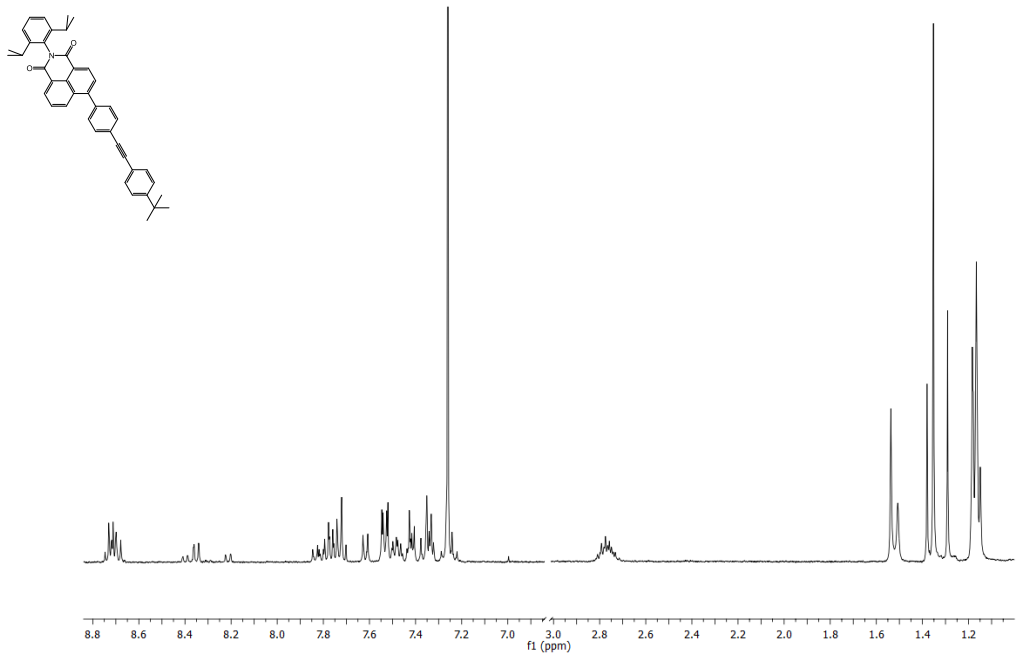

^{1}H NMR (400 MHz, $CDCl_3$): δ (ppm) 8.75-7.2 (m, 16H), 1.55-1.15 (m, 21H)

Compound **15**

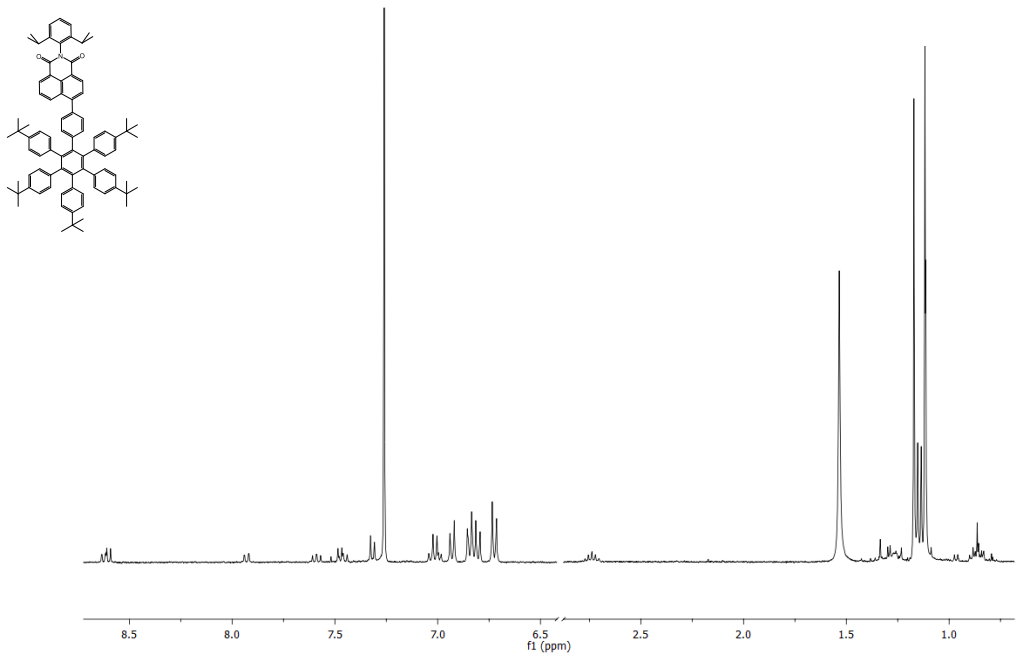

^{1}H NMR (400 MHz, $CDCl_3$): δ (ppm) 8.61 (dd, J = 9.2, 7.4 Hz, 2H), 7.93 (d, J = 8.6 Hz, 2H), 7.62-7.55 (m, 2H), 7.46 (dd, J = 10.1, 7.6 Hz, 2H), 7.32 (d, J = 7.7

Hz, 2H), 7.01 (q, J = 8.3 Hz, 2H), 6.93 (d, J = 8.4 Hz, 2H), 6.87-6.78 (m, 4H), 6.72 (d, J = 8.4 Hz, 2H), 2.77-2.68 (m, 1H), 1.53-1.0 (s, 57)

Compound **16**

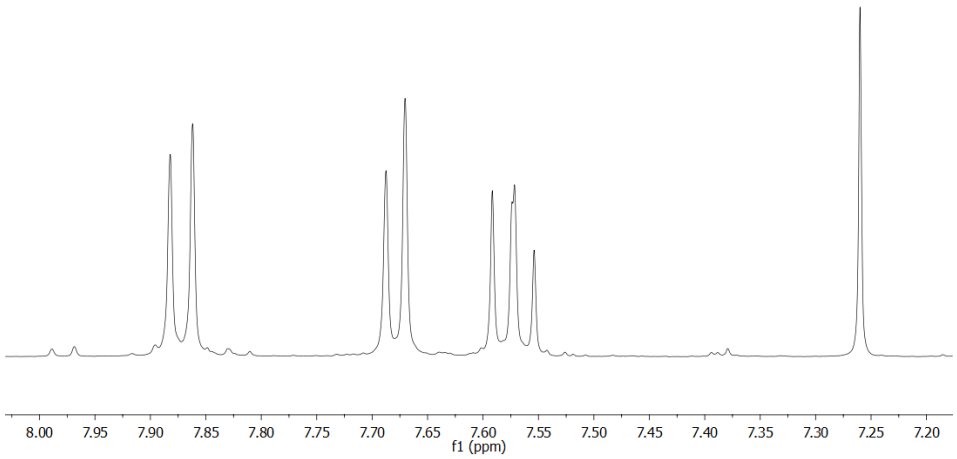

^{1}H NMR (400 MHz, $CDCl_3$): δ (ppm) 7.87 (d, J = 8.1 Hz, 2H), 7.68 (d, J = 6.9 Hz, 2H), 7.57 (dd, J = 8.0, 7.1 Hz, 2H)

Compound **17**

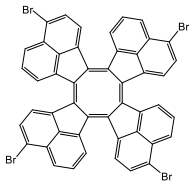

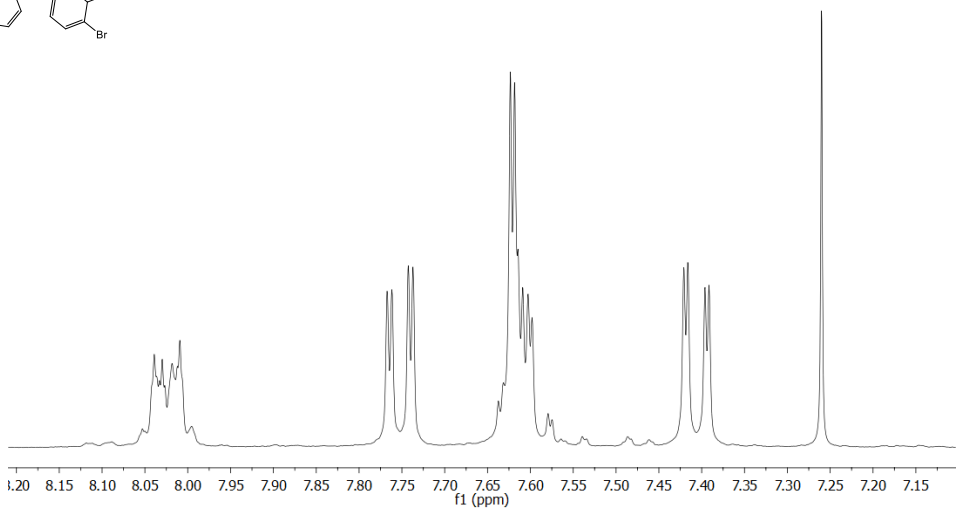

^{1}H NMR (400 MHz, $CDCl_3$): δ (ppm) 8.05-8.00 (m, 1H), 7.75 (dd, J = 7.4, 1.6 Hz, 1H), 7.65-7.59 (m, 2H), 7.41 (dd, J = 7.4, 1.4 Hz, 1H)

MALDI-TOF Mass Spectrometry

Compound **1**

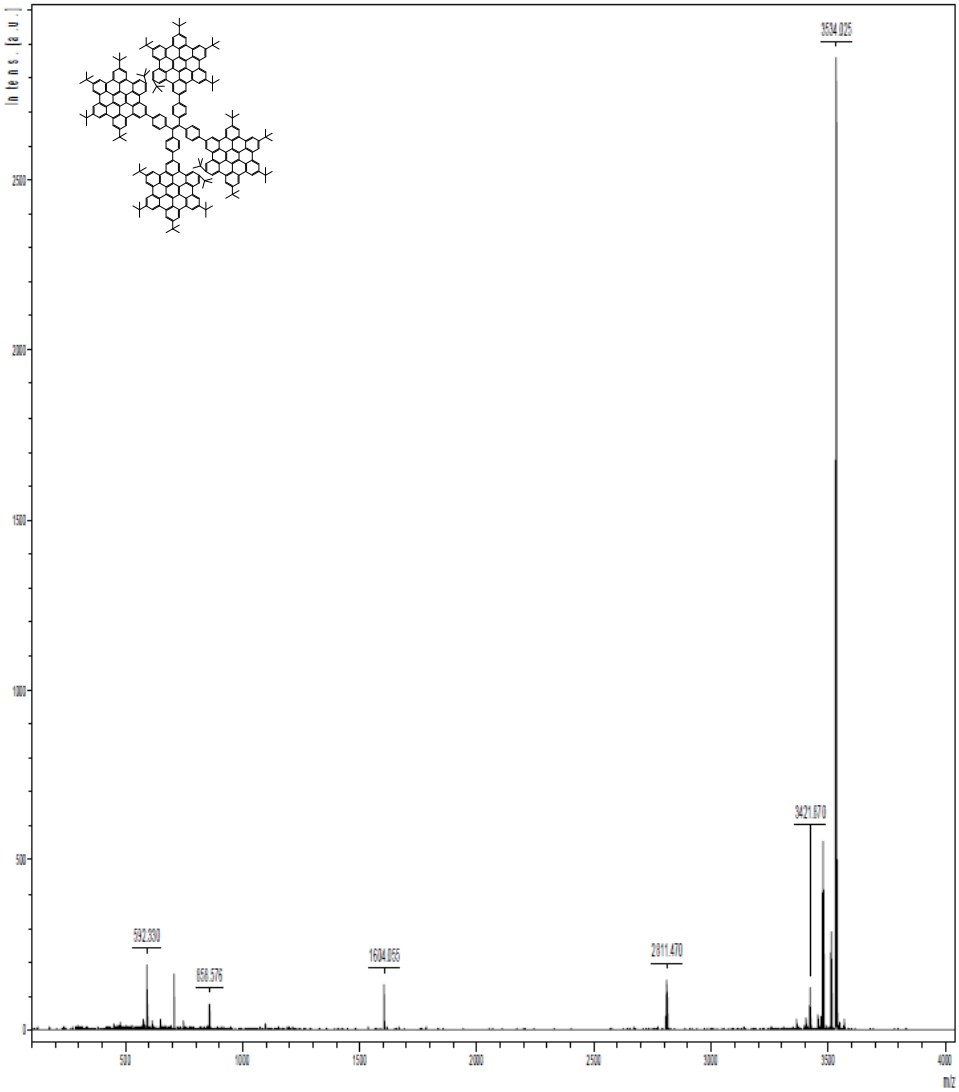

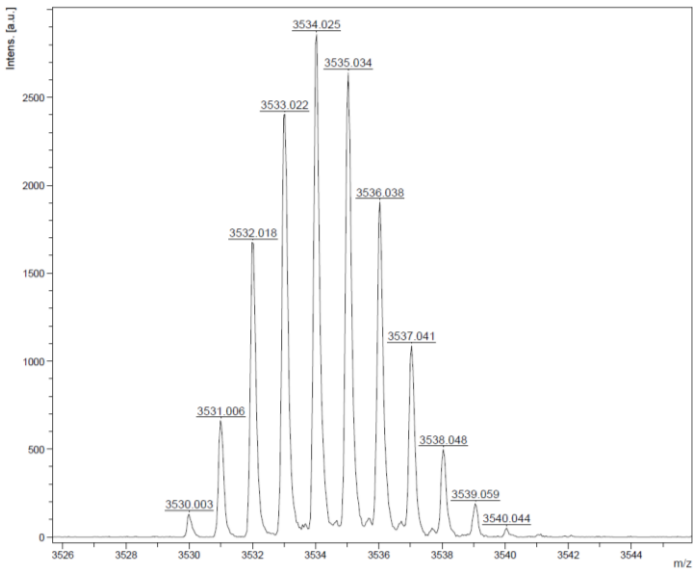

Compound **2**

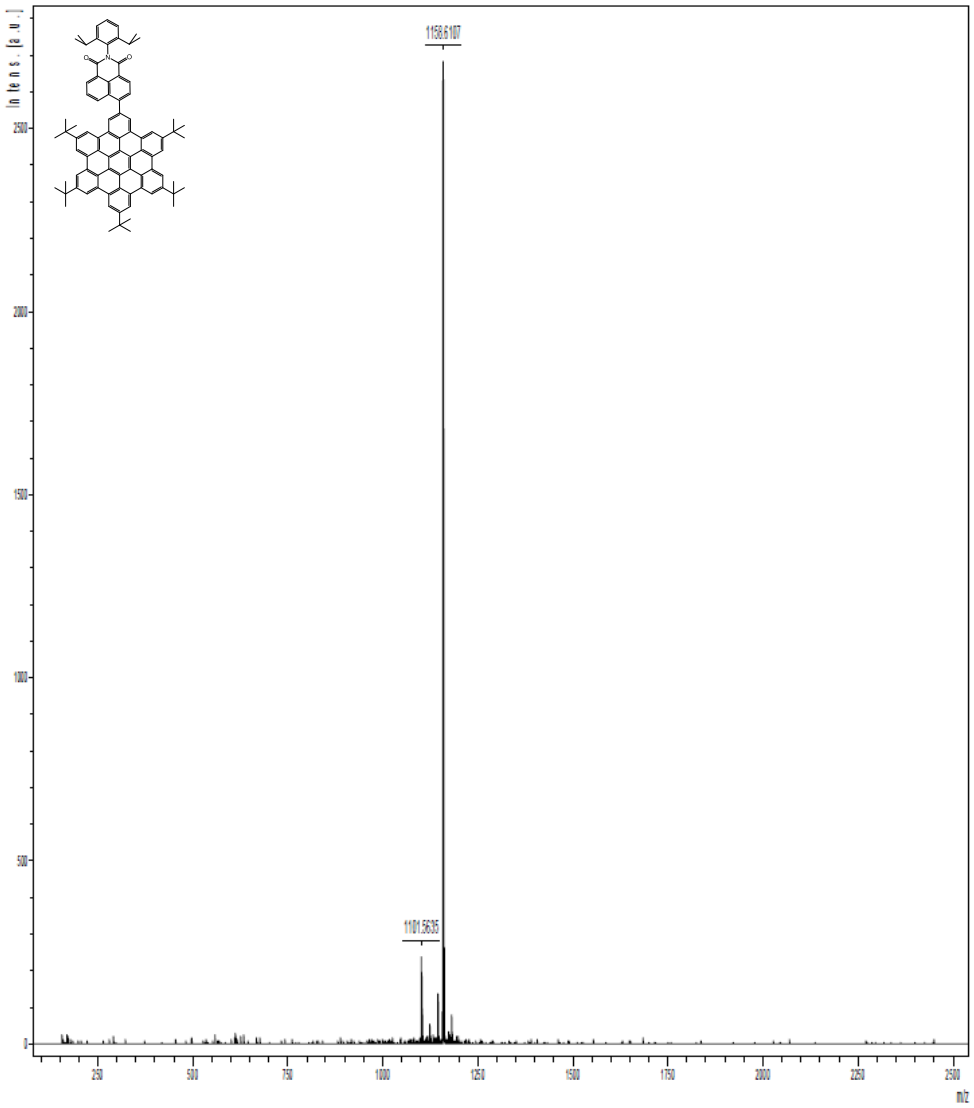
1158.6107
1101.5635
Intens. [a.u.]
m/z

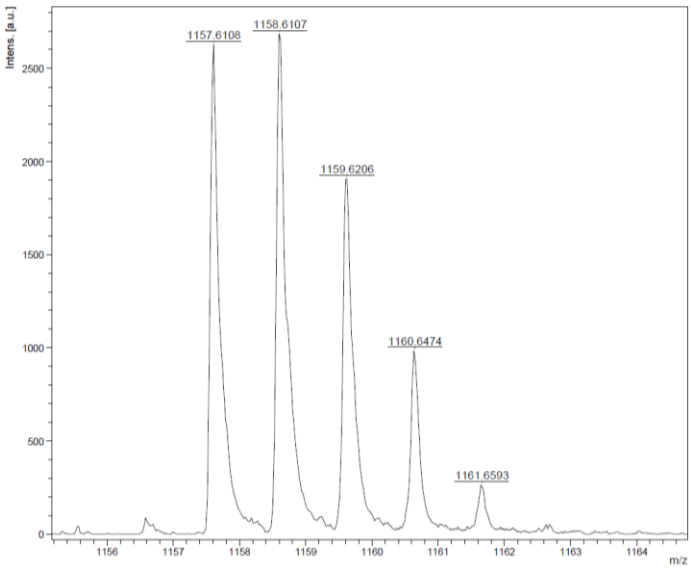
1157.6108
1158.6107
1159.6206
1160.6474
1161.6593
Intens. [a.u.]
m/z

Compound **3'**

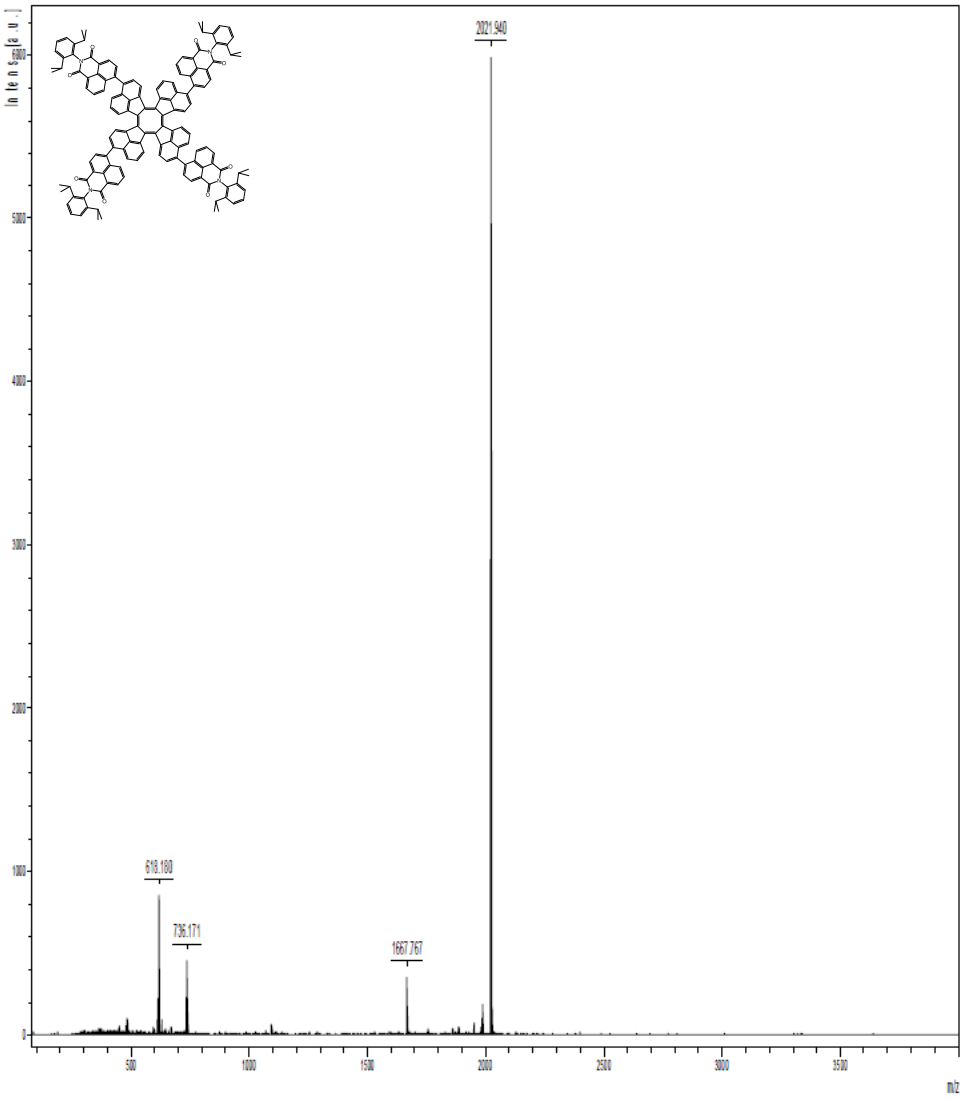

Compound **6**

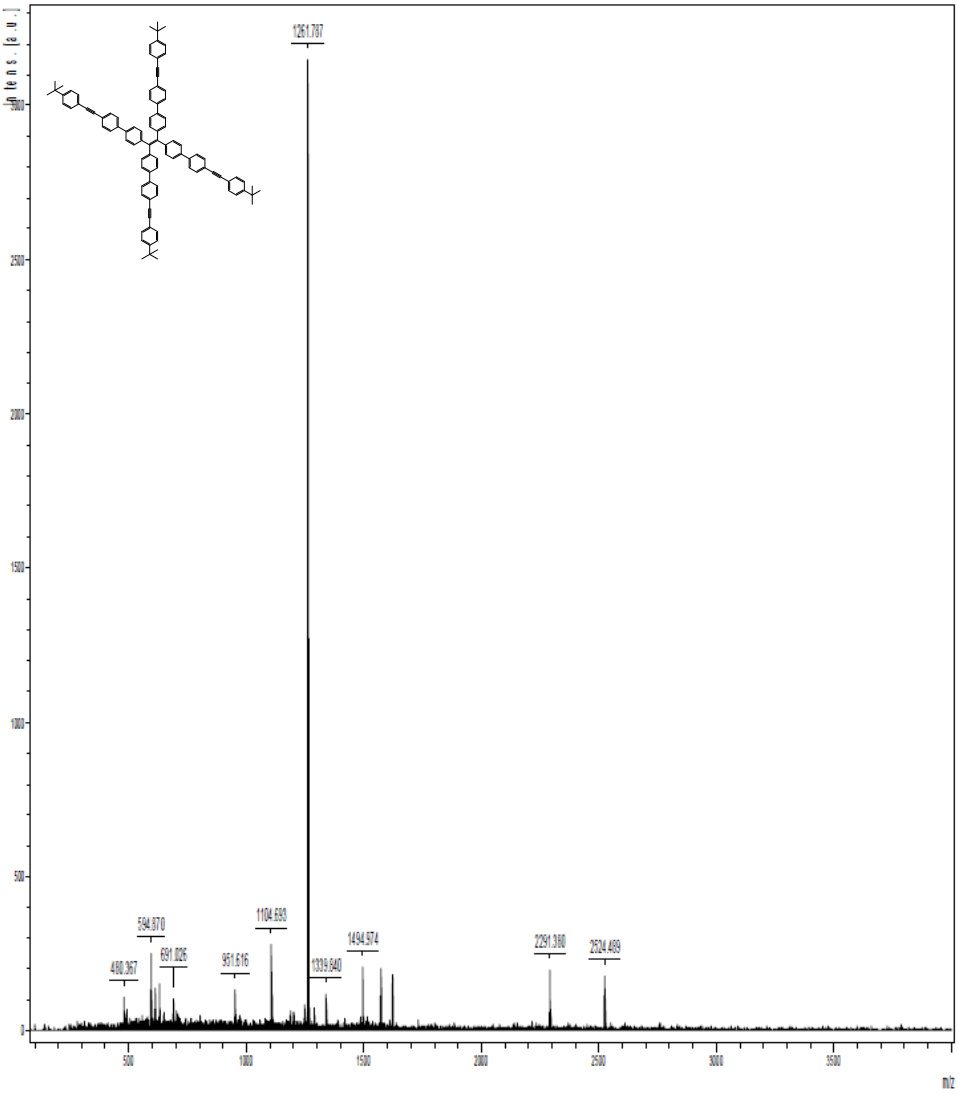
Intens. [a.u.]
1261.787
594.670
691.805
1104.680
951.616
1339.640
1494.974
2291.398
2524.499
m/z

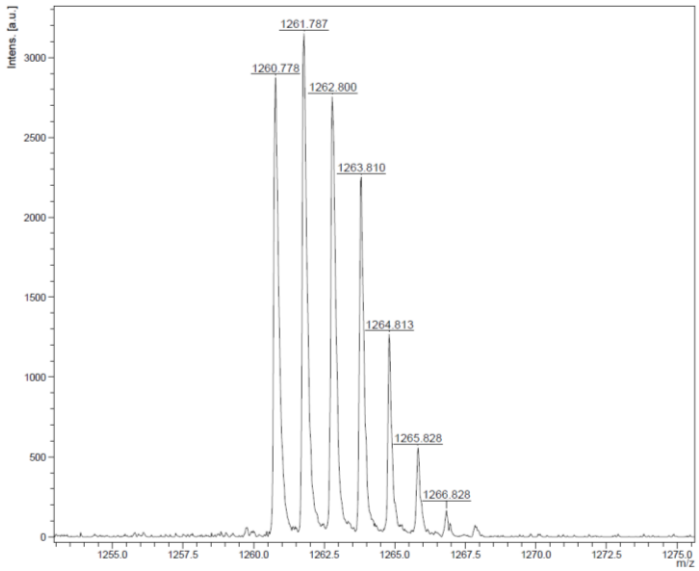
Intens. [a.u.]
1261.787
1260.778
1262.800
1263.810
1264.813
1265.828
1266.828
m/z

Compound **11**

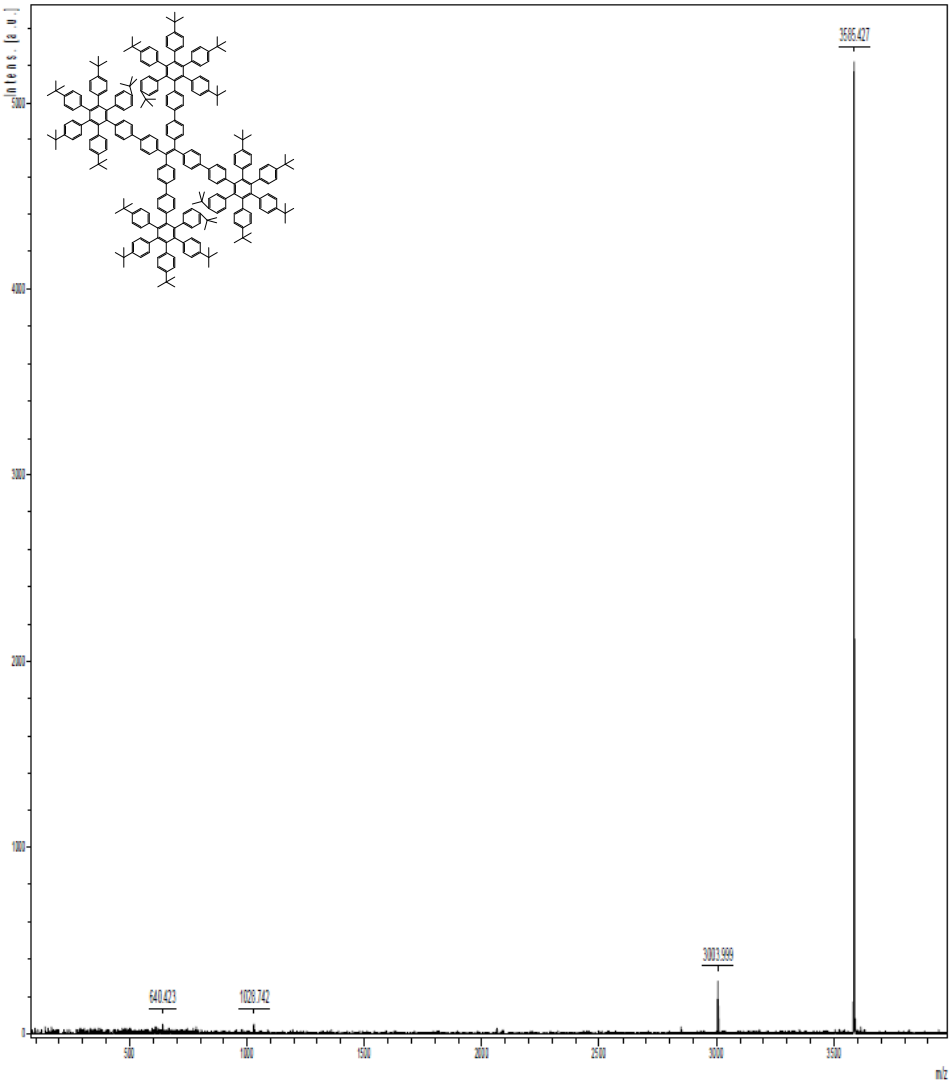
Intens. [a.u.]
3585.427
3003.999
640.423
1026.742
m/z

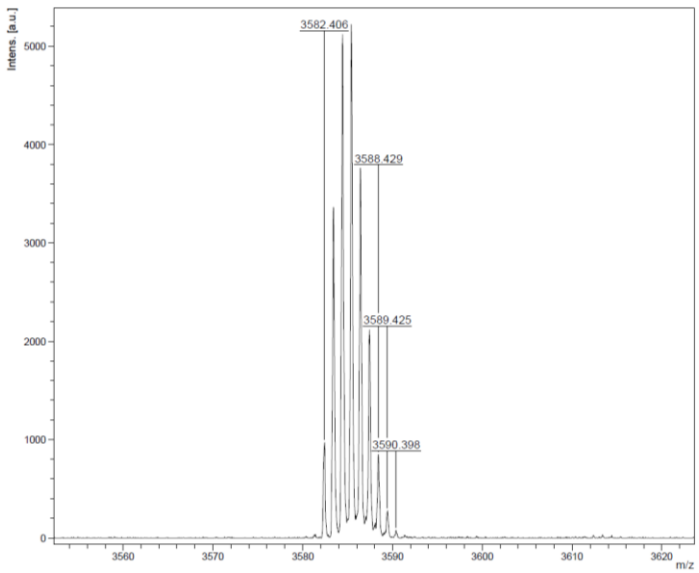
Intens. [a.u.]
3582.406
3588.429
3589.425
3590.398
m/z

Compound **15**

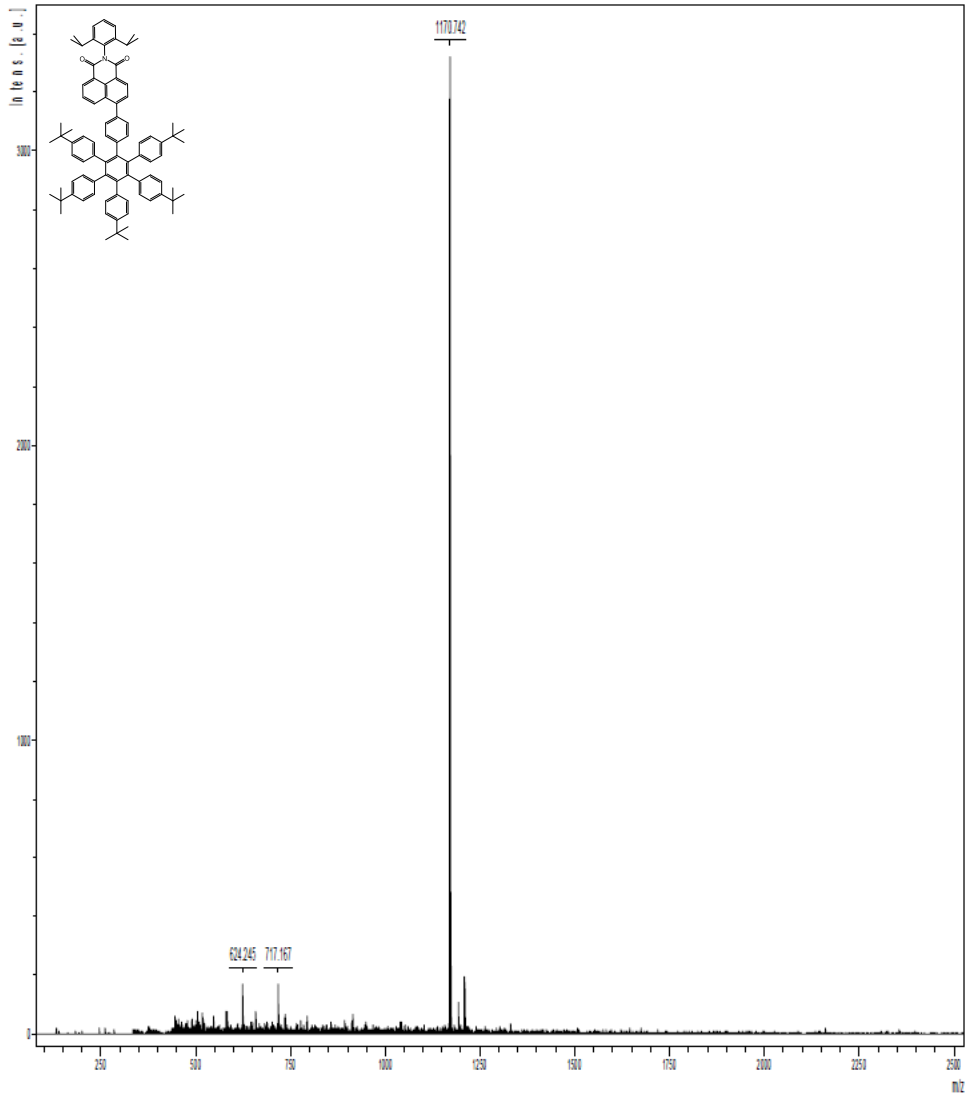
1170.742
624.245
717.167
Intens. [a.u.]
m/z

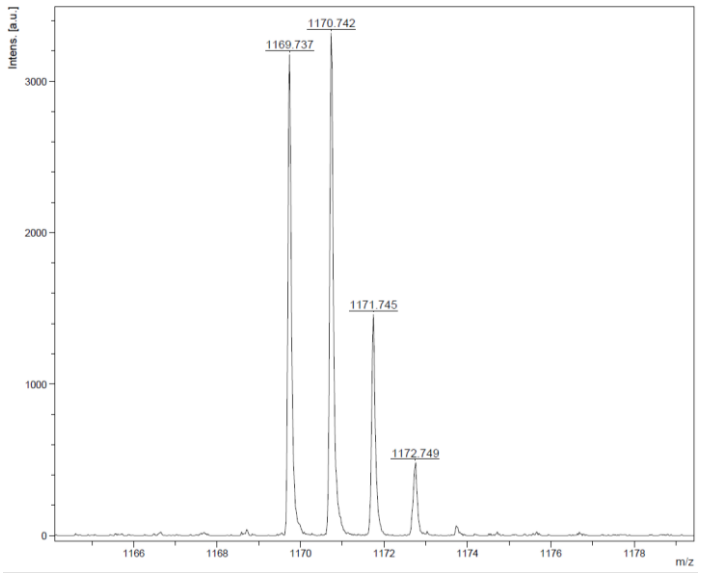
1170.742
1169.737
1171.745
1172.749
Intens. [a.u.]
m/z

Acknowledgements

With this thesis project I had the opportunity to experience a new world, working in a so advanced and stimulating environment, learning more than I would ever expected.
In Madrid, I found a beautiful and cohesive group full of passionate and interested scientists and people.
For all this, I want to thank Professor Nazario Martín León for accepting me and for pushing all the group beyond their limits and the limits of science.
Furthermore, I want to thank Professor Enzo Menna for giving me the chance to leave Italy and making me discover this fascinating field of chemistry.

I want to give a special thanks to Doctor Javier Urieta-Mora that led me through this experience and, equally important, suggested me the best places to eat in Madrid.